creative commons
COMMONS DEED

저작자표시-비영리-변경금지 2.0 대한민국

이용자는 아래의 조건을 따르는 경우에 한하여 자유롭게

- 이 저작물을 복제, 배포, 전송, 전시, 공연 및 방송할 수 있습니다.

다음과 같은 조건을 따라야 합니다:

저작자표시. 귀하는 원저작자를 표시하여야 합니다.

비영리. 귀하는 이 저작물을 영리 목적으로 이용할 수 없습니다.

변경금지. 귀하는 이 저작물을 개작, 변형 또는 가공할 수 없습니다.

- 귀하는, 이 저작물의 재이용이나 배포의 경우, 이 저작물에 적용된 이용허락조건을 명확하게 나타내어야 합니다.
- 저작권자로부터 별도의 허가를 받으면 이러한 조건들은 적용되지 않습니다.

저작권법에 따른 이용자의 권리는 위의 내용에 의하여 영향을 받지 않습니다.

이것은 이용허락규약(Legal Code)을 이해하기 쉽게 요약한 것입니다.

Disclaimer

dCollection

이학석사 학위논문

Changes of Prokaryotic Communities in Biofilm Formation on Microplastics in Coastal Seawaters

해양 미세플라스틱 생물막 형성 과정에서 원핵생물 군집 구조 변화 연구

2023 년 8 월

서울대학교 대학원

지구환경과학부

홍 연 우

Changes of Prokaryotic Communities in Biofilm Formation on Microplastics in Coastal Seawaters

해양 미세플라스틱 생물막 형성 과정에서 원핵생물 군집 구조 변화 연구

지도 교수 황 청 연

이 논문을 이학석사 학위논문으로 제출함

2023 년 5 월

서울대학교 대학원

지구환경과학부

홍 연 우

홍 연 우의 이학석사 학위논문을 인준함

2023 년 7 월

위 원 장 정 해 진 (인)

부위원장 황 청 연 (인)

위 원 김 종 성 (인)

Abstract

Plastic debris is rapidly colonized by diverse microorganisms, providing microbial niches in marine biota. Previous investigations have been conducted on microbial communities of microplastics collected from the environment, and the results were diverse. These results suggested that microplastics could be influenced by exposure time. Moreover, prokaryotic communities in the initial stages of microplastic biofilm formation remain poorly understood. In this study, we investigated the initial stages (Day 1–14) of prokaryotic communities on five polymer types exposed for different time periods in coastal seawater using in situ incubation. Next–generation amplicon sequencing based on the 16S rRNA gene was used to reveal the prokaryotic composition of the biofilm formation on microplastics, depending on the exposure time and polymer type. The microplastic-associated prokaryotic communities exhibited distinct community composition and structure, clearly differentiating them from the bulk seawater communities. The microplastic-associated prokaryotic communities were influenced by exposure time rather than polymer types based on Bray-Curtis dissimilarity distance. Furthermore, the analysis revealed that the microplastic samples exhibited a higher abundance of amplicon sequence variants (ASVs) associated with obligate hydrocarbonoclastic bacteria (OHCB) compared to the seawater samples. Additionally, specific ASVs were observed depending on the types of polymers present in the microplastics. Moreover, the relative abundances of major taxa in microplastic communities exhibited temporal variations. The results revealed that the initial prokaryotic communities showed dynamic characteristics, characterized by fluctuations in composition and structure. In addition to,

microplastic-associated functions of benzoate degradation and polycyclic aromatic hydrocarbon (PAH) degradation represented that microplastic communities exhibited an increase in these functions over time. This study offers insights into the formation of microplastic biofilms during the initial stages and establishes a baseline for understanding the mechanisms underlying microbial microplastic biofilm formation. Furthermore, our research could provide fundamental knowledge to support further study on marine microplastic pollution.

Keywords: Microplastic, Early biofilm, Prokaryotic community, In situ experiment, Amplicon sequencing

Student Number: 2021-20686

Table of Contents

Abbreviations

ANOSIM	Analysis of similarities
ASV	Amplicon Sequence Variant
FL	Free-living
GPPS	General Purpose Polystyrene
HDPE	High-Density Polyethylene
HIPS	High Impact Polystyrene
KEGG	Kyoto Encyclopedia of Genes and Genomes
KO	KEGG Ortholog
LDA	Linear Discriminant Analysis
LDPE	Low-Density Polyethylene
LEfSe	Linear Discriminant Analysis Effect Size
MP	Microplastic
OHCB	Obligate Hydrocarbonoclastic Bacteria
NMDS	Non-metric multidimensional scaling
PA	Particle-attached
PCoA	Principal coordinates analysis
PCR	Polymerase Chain Reaction
PE	Paired-End
PERMANOVA	Permutational multivariate analysis of variance
PICRUSt2	Phylogenetic Investigation of Communities by Reconstruction of Observed States
PP	Polypropylene
SW	Seawater

List of Tables

List of Figures

1. Introduction

Plastic litter is a global environmental concern, particularly in the oceans where it poses a significant threat to marine ecosystems. In 2018, global plastic resin production rose to 359 million metric tons (PlasticsEurope 2019). As a result, it is estimated that from 5.5 to 14.5 million metric tons of plastic waste might have been discharged into the oceans during that year (PlasticsEurope 2019; Wayman & Niemann 2021). As plastic debris enters the marine environment, it undergoes physical and chemical weathering processes, ultimately forming microplastics, which range from 1 μm to 5 mm in size (Frias & Nash 2019). These microplastics are present in diverse marine environments, including coastal seawater, sediment, open water, and even deep sea or polar regions with minimal human impact (Auta et al. 2017).

The "Plastisphere", which refers to the diverse microbial communities that colonize on plastic debris (Zettler et al. 2013), provides microbial niches for marine biota. Moreover, the ability to form biofilm offers numerous advantages to microorganisms, including higher accessibility to nutrients, protection from UV radiation, maintenance of extracellular enzyme activities, and survival from predation (Dang & Lovell 2000, 2016). Also, plastisphere microbial communities are clearly differentiated from the surrounding seawater (Basili et al. 2020; Frère et al. 2018; Zettler et al. 2013; Zhang et al. 2022). Previous studies were conducted on factors affecting plastisphere microbial communities in field incubation systems. Zhang et al. (Zhang et al. 2022) investigated the microbial community dynamics for different polymer types at timepoints of 1, 4, and 8 weeks in field incubation

experiment. This previous study confirmed that the plastisphere microbial communities were influenced by polymer types, exposure time, and environmental factors. In addition, the bacterial communities on microplastics were found to be significantly varied depending on marine habitat and exposure duration, rather than polymer types (Li et al. 2020). However, there is no significance in bacterial communities with polymer types (PE and PP) and exposure time (Dudek et al. 2020). Hou et al. (Hou et al. 2021) conducted prokaryotic microplastic communities for three polymer types (PE, PP, and PET) across different exposure times (Day 15, 30, 60, and 90) in a mariculture cage. The distinct prokaryotic communities were observed to form on different types of microplastics. Additionally, the dissimilarity in the prokaryotic communities between microplastics and surrounding water fractions tended to decrease over time. Latva et al. (Latva et al. 2022) carried out field incubations to examine the prokaryotic and eukaryotic community structures during very early stages (15 min, 4 h, 6 h, 28 h, and 76 h) and they found that exposure time significantly impacted the prokaryotic and eukaryotic communities. This study, though, had a lack of comparison to surrounding seawater and only examined a single polymer type in the experimental setup. The initial stages of biofilm formation on marine submerged substrates are highly dynamic (Dang & Lovell 2000; Latva et al. 2022; Pollet et al. 2018). However, prokaryotic community succession remains poorly understood especially during the initial stages of microplastic biofilm formation, compared to surrounding seawater.

In this study, we investigated the initial stages (Day 1–14) of prokaryotic communities on five different types of microplastics (low-density polyethylene, high-density polyethylene, general-purpose polystyrene, high-impact polystyrene,

and polypropylene) exposed for different time periods in coastal seawater using in situ incubation. Hence, this study aimed (1) to find the differences between microplastic-associated prokaryotic communities and bulk seawater communities and (2) to characterize the prokaryotic communities during the initial stages of microplastic biofilm formation in coastal seawater.

2. Materials & Methods

2.1. Experimental Setup and Sampling Procedures

The in situ incubation experiment and bulk seawater sampling were conducted on the coast near Hari Port in Busan, Republic of Korea (35°04' 33" N, 129°05' 00" E) (Figure 1), on October 11th, 2022, and October 25th, 2022.

The five polymer types of microplastics used in the experiment were GPPS, HIPS, LDPE, HDPE, PP (Polypia, Republic of Korea). The size of the microplastic pellets was between 2 and 5 mm. Prior to the experiment, the polymer types of microplastics were analyzed by Nicolet™ iN10 MX Infrared Imaging Microscope (Thermo Fisher Scientific, USA) to confirm the polymer types (Figure 2). The microplastics were washed twice in 70 % ethanol and sterilized distilled water. The microplastics were stored in sterilized bags until in situ incubation experiment. The microplastic pellets were placed separately for each polymer type in a sterilized cylindrical-shaped stainless steel cage (mesh size, 1.2 mm; diameter, 19.5 cm; height, 19.5 cm). Five stainless steel cages containing different microplastic pellets were connected to the buoy using stainless steel ropes and the cages were submerged at approximately 0.5–2 m in depth. A schematic of the experimental design is shown in Figure 3. The microplastics were conducted in situ experiment for 14 days.

These microplastics were subsampled at different time points (Day 1, 2, 3, 5, 6, and 14) in coastal seawater. The stainless steel cage containing PP was lost on the Day 14, hence, there was no data for Day 14 of PP. At each time point, approximately 15 g of each polymer type was collected in a 50 ml conical tube with triplicate and

rinsed loosely 2–3 times with 0.2 μm filtered sterile 3 % NaCl to remove bulk seawater. Afterward, the 50 ml conical tubes containing microplastic samples were filled with 40 ml of 0.2 μm filtered sterile 3 % NaCl. The microplastic-attached prokaryotes were collected by 0.2 μm filtration after oscillation step using Vortex-Genie 2 (Scientific Industries, USA) for 30 minutes at 3,200 rpm. This modified method was adopted based on the techniques described in previous studies (Wen et al. 2020; Zhang et al. 2022). To retrieve residual prokaryotes, 40 ml of 0.2 μm filtered sterilized 3 % NaCl was put into the 50 ml conical tube once more and shaken to filter on the same 0.2 μm filter.

The bulk seawater was collected near the experiment area of the microplastic in situ incubation. The raw seawater samples (1.5–2.2 L) were filtered triplicate with a 3.0 μm pore-sized polycarbonate membrane filter (47 mm, Millipore) to detect the particle-attached prokaryotes. The filtrate was filtered triplicate by a 0.2 μm pore-sized polycarbonate membrane filter (47 mm, Millipore) to collect free-living prokaryotes. All filter samples were stored at −80 ℃ until further analysis.

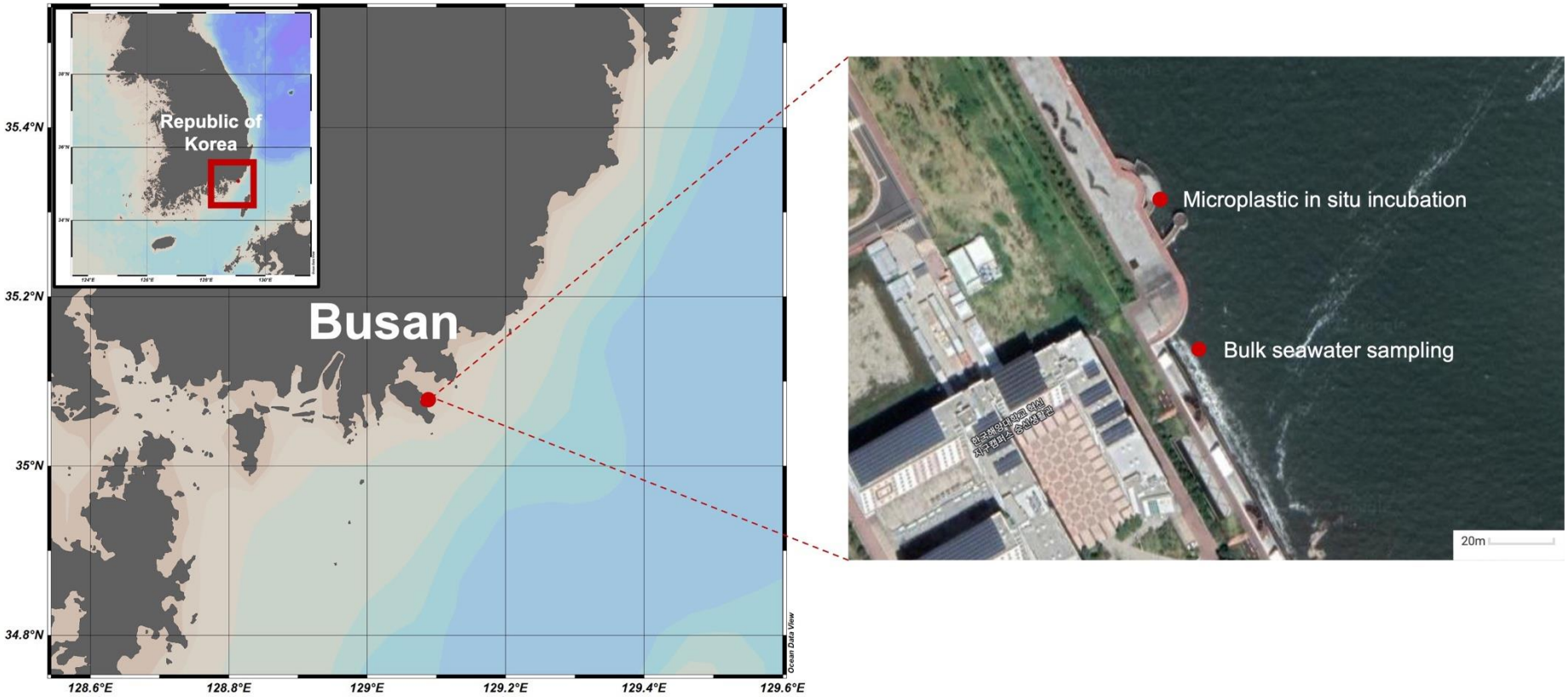

Figure 1. Location of microplastic in situ incubation experiment and bulk seawater sampling in the Southern Sea of Korea (from Ocean Data View [version 5.3.0, https://odv.awi.de/] and Google Maps).

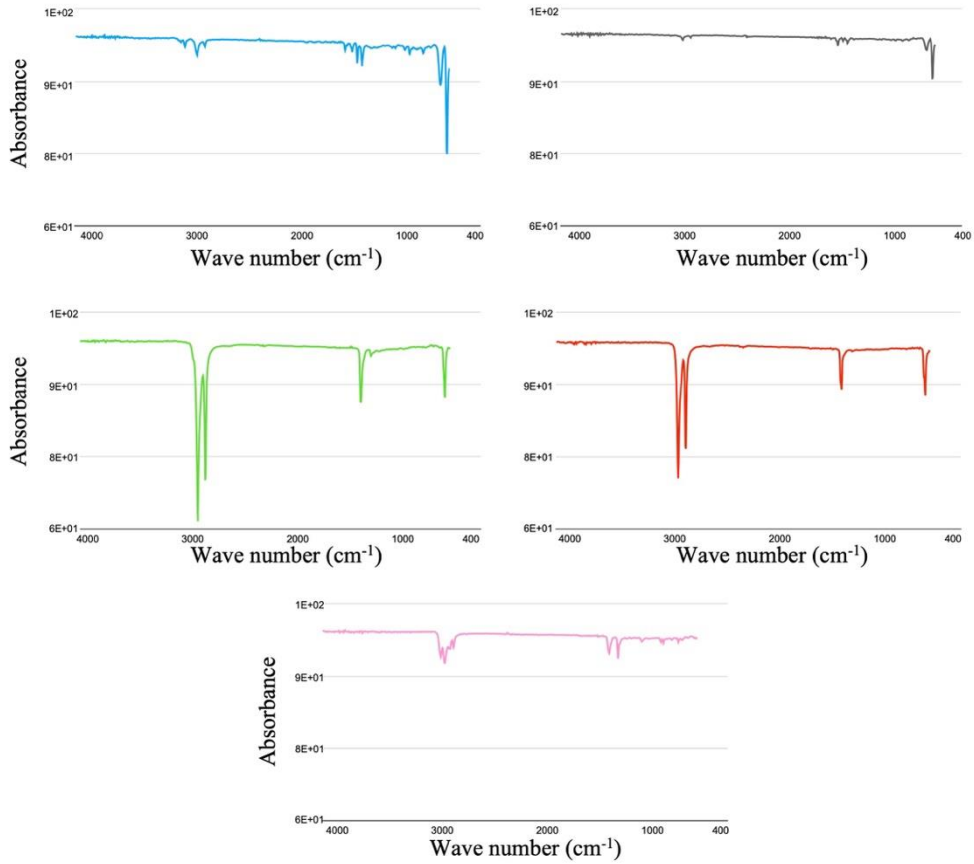

Figure 2. FT-IR (Fourier transform infrared) spectra of the different microplastics.

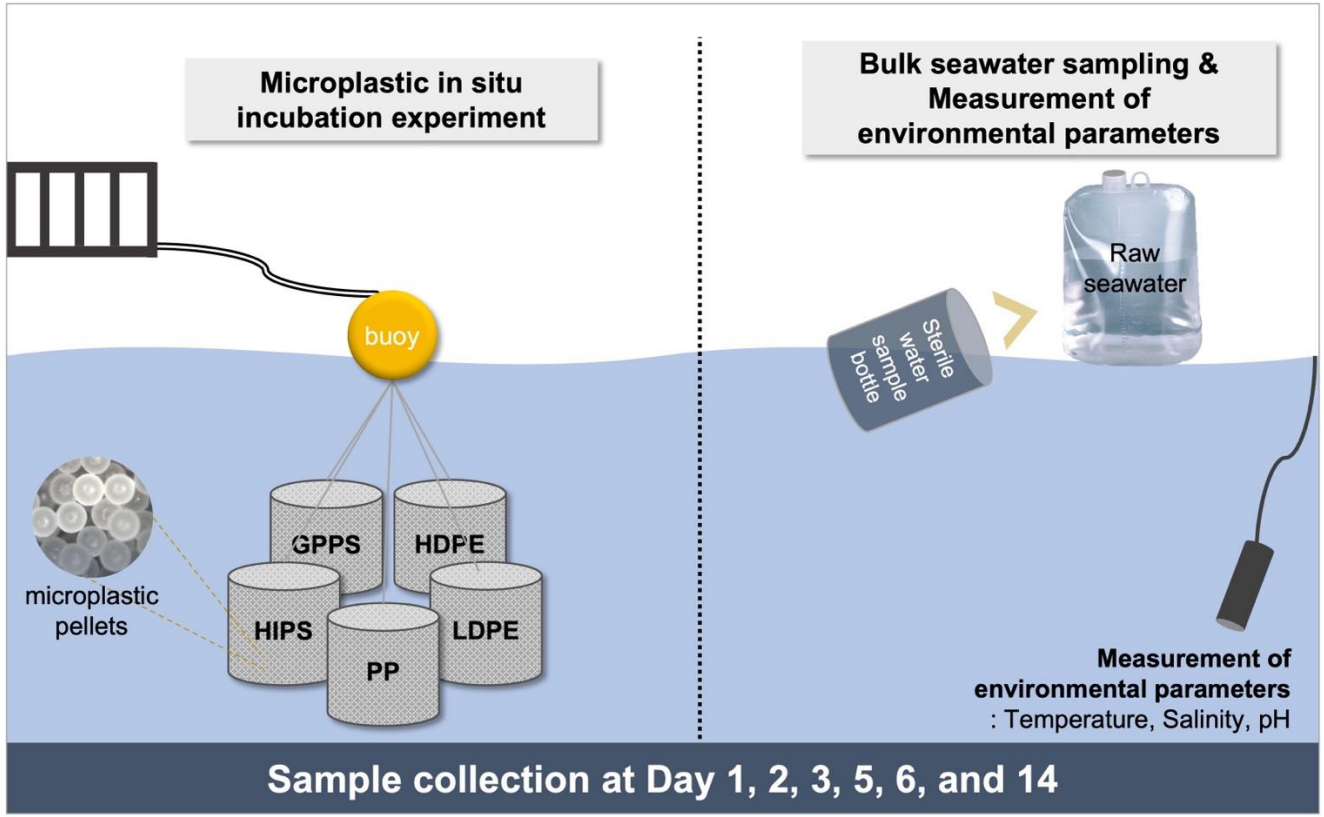

Figure 3. Schematic of experimental design. Microplastic pellet subsampling and bulk seawater sampling were conducted on the same day. Environmental parameters (temperature, salinity, and pH) were measured in situ.

2.2. Prokaryotic Abundance and Environmental Parameters

10 ml of the raw bulk seawater was stored at −20 ℃ supplemented with 0.02 μm filtered formalin (final concentration 2 %) for the prokaryotic abundance. A volume of 700 μl of the fixed raw bulk seawater was filtered through a 0.02 μm Anodisc filter (25 mm, Whatman). Subsequently, the Anodisc filters were carefully placed on a drop of 100 μl of diluted SYBR Gold (2.5 % of final concentration). (Shibata et al. 2006). This step was performed in the dark condition for 15 minutes. The abundance of prokaryotic cells was observed and counted using epi-fluorescence microscopy (BX60, Olympus).

Environment parameters, including temperature, salinity, (YSI, USA) and pH of seawater were measured in triplicate in situ at each time point. For chlorophyll *a* measurement, 2–2.2 L of seawater were filtered in duplicate by GF/F filters on Day 1, 5, and 14. After filtration, the GF/F filters were stored at -20 ℃ until before analysis. The extraction and calculation of chlorophyll *a* were followed as the methods (Parsons et al. 1984). The nutrient concentration of bulk seawater was measured in triplicate using the QuAAtro AutoAnalyzer (SEAL Analytical, USA). A duplicated subsample of 40 ml stored at −20 ℃ was used for the analysis. The measured macronutrients encompassed ammonium (NH_4), nitrite plus nitrate (NO_2+NO_3), phosphate (PO_4), and silicate (SiO_2). To investigate the correlation between environmental parameters including temperature, pH, salinity, ammonium (NH_4), nitrite plus nitrate (NO_2+NO_3), phosphate (PO_4), and silicate (SiO_2) and the dominant taxa (top 10) of microplastic samples, we calculated Spearman correlation coefficients. The correlation results with environmental parameters were visualized using ‘corrplot’ package version 0.92 (Wei & Simko 2021) in R.

2.3. DNA Extraction, Amplicon Sequencing, and Data Processing

The genomic DNA of the filter samples was extracted using the DNeasy Power Soil Kit (Qiagen) according to the manufacturer's instructions. The concentration of genomic DNA was quantified using NanoDrop spectrophotometers (Thermo Fisher Scientific, USA). The 16S rRNA gene V4–V5 hypervariable region was amplified using PCR Master Mix (Biofact, Republic of Korea) and barcoded 515F (5'–GTGYCAGCMGCCGCGGTAA–3') 926R (5'–CCGYCAATTYMTTTRAGTTT–3') primers (Parada et al. 2016; Vaksmaa et al. 2021). The PCR product was purified using HiGene™ Gel & PCR Purification System (Biofact, Republic of Korea). The purified PCR product was quantified using NanoDrop spectrophotometers. The PCR products were pooled to an equimolar amount. The library was constructed with the Nextera XT index Kit (Illumina, USA) and sequenced by Illumina MiSeq PE (Paired-End) at LAS, Republic of Korea.

The quality of the raw amplicon sequences was assessed by FastQC version 0.11.9 (Andrews 2010). Trimming of adaptors was processed by Trimmomatic version 0.39 (Bolger et al. 2014). The barcoded sequences were demultiplexed with Cutadapt version 4.2 (Martin 2011). The demultiplexed sequences were denoised using DADA2 (Callahan et al. 2016) via Qiime2 (https://docs.qiime2.org/2022.11/) (Bolyen et al. 2019). The taxonomic assignment of the amplicon sequence variants (ASVs) was performed using Naive Bayes classifier trained on Silva 138 99% OTUs full-length sequences (Bokulich et al., 2018). After the taxonomic assignment, the sequences classified as Chloroplast, Eukaryota, Mitochondria, and Unassigned were exclude.

2.4. Statistical Analysis

Sequencing depth of all samples was visually evaluated through rarefaction curves using the ‘diversity alpha-rarefaction’ function in Qiime2 (Bolyen et al. 2019). Subsequent statistical analyses were conducted in R version 4.2.2 (RCoreTeam 2022). Alpha diversity indices, such as Chao1, Inverse Simpson, Shannon, and ACE were calculated using phyloseq package version 1.42.0 (McMurdie & Holmes 2013) in R. For groups with significant differences, pairwise Wilcoxon tests with Bonferroni corrections were applied to account for multiple comparisons after Shapiro-Wilk normality test using stats package in R. Beta diversity was analyzed by Principal Coordinates Analysis (PCoA) plots based on Bray-Curtis dissimilarities using Phyloseq package. The significance of pairwise differences in prokaryotic community composition was assessed using the Analysis of Similarity (ANOSIM) method, implemented through the vegan package (Oksanen & Jari, 2020) and the 'diversity beta-group-significance' command in Qiime2, with 999 permutations. The selection of major ASVs (Amplicon Sequence Variants) was based on their presence in at least one microplastic sample and a minimum composition threshold of 4%. The linear discriminant analysis effect size (LEfSe) analysis was conducted using an online tool within the Galaxy to identify marker species among the groups (Segata et al. 2011) and Linear Discriminant Analysis (LDA) score value was 2.0. All other plots were visualized by ggplot2 package (Wickham & Wickham 2016) in R.

2.5. Functional Inference

PICRUSt2 (Phylogenetic Investigation of Communities by Reconstruction of Observed States) plugged in Qiime2 was used for the prediction of functional inference of the prokaryotic communities (Douglas et al. 2020). The pathway abundance tables containing the Kyoto Encyclopedia of Genes and Genomes (KEGG) Orthologs (KOs) were acquired using the Qiime2 ‘full-pipeline’ function (PICRUSt2 Tutorial, version 2.5.2). In the analysis, the KEGG Orthologs (KOs) were assigned to level 3 KEGG pathways using the KEGG BRITE hierarchy. The abundance values of KEGG pathways were normalized to relative abundance to compare among groups and exposure times.

3. Results

3.1. Prokaryotic Abundance of Bulk Seawater and Environmental Parameters

The prokaryotic abundance of bulk seawater samples ranged from 3.73–7.74 $\times 10^5$ ml^{-1}, with the lowest abundance detected on Day 6 (Table 1 and Figure 4). The results of environmental parameters were shown in Table 1 and Figure 4. For 14 days, the mean range of the temperature, salinity, pH, and Chlorophyll *a* concentration were 18.40–20.77 ℃, 31.50–32.37, 8.11–8.20, and 0.076–0.179, respectively. Notably, on Day 14, the lowest values of temperature and Chlorophyll *a* concentration were observed.

Table 1. The results of the environmental parameters and prokaryotic abundance. NA; not available (Mean±SD)

Date (yyyy/mm/dd)	Time point	Temperature (℃)	Salinity (ppt)	pH	Chlorophyll *a* ($\mu g/l^{-1}$)	Prokaryotic abundance ($\times 10^5\ ml^{-1}$)
2022/10/12	Day 1	20.23±0.06	31.73±0.06	8.11±0.02	0.163±0.003	7.74±0.05
2022/10/13	Day 2	19.83±0.15	31.87±0.15	8.15±0.02	NA	7.20±0.05
2022/10/14	Day 3	20.07±0.12	31.50±0.10	8.13±0.03	NA	6.31±0.04
2022/10/16	Day 5	20.77±0.06	31.53±0.06	8.17±0.02	0.179±0.010	7.11±0.05
2022/10/17	Day 6	20.57±0.21	31.70±0.44	8.20±0.01	NA	3.73±0.03
2022/10/25	Day 14	18.40±0.00	32.37±0.06	8.14±0.01	0.076±0.027	4.39±0.03

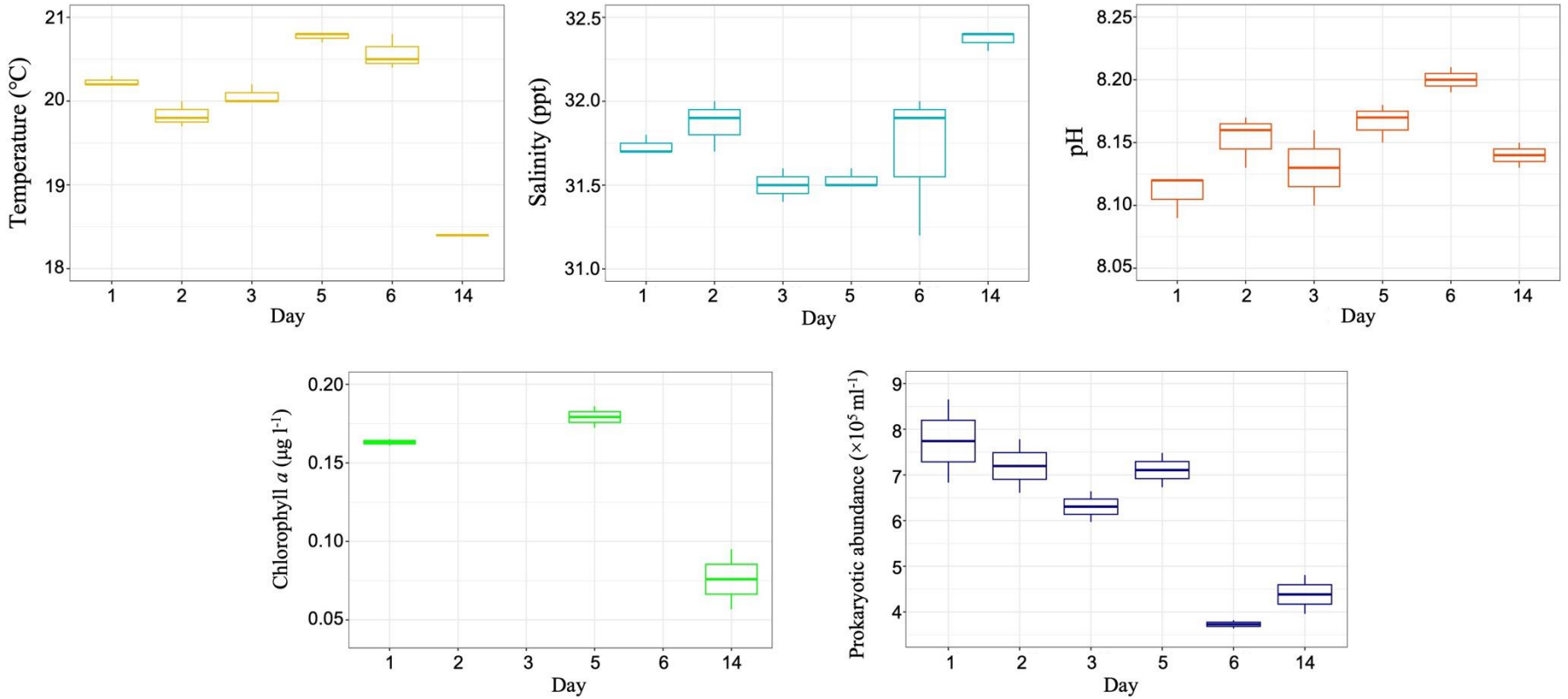

Figure 4. The boxplots of the environmental parameters and prokaryotic abundance. Chlorophyll *a* analysis was conducted only on Day 1, Day 5, and Day 14.

3.2. Diversity of Prokaryotic Communities

3.2.1. Sequencing Results

A total of 6,291,476 raw reads were obtained for analysis. A total of 3,144,622 high–quality reads from 122 samples were retrieved after quality filtering, trimming, denoising, and taxa filtering (Table 2). Additionally, 12,297 ASVs were observed among all 122 samples. Furthermore, the frequency distribution of the dataset was as follows: The minimum frequency observed was 1,592, indicating the lowest occurrence of a specific event. The median frequency was 18,877, indicating that 50% of the data points had a frequency equal to or lower than this value. The mean frequency was calculated to be 25,776, providing an overall average value for the frequencies observed.

All 122 samples yielded rarefaction curves with a plateau (Figure 5), showing sufficient sequence depth.

Table 2. Number of reads at each quality control (QC) stage. The total number of high-quality reads in the study was determined to be 3,144,622. (Mean±SD)

Sample ID	Raw reads	Denoising	Merging	Removal of chimera	Taxa filtering
GPPS-D01	16225±4417	13088±3886	8261±1855	7526±2065	6102±1057
GPPS-D02	16758±9502	13719±9077	11004±7899	10318±7475	9591±6971
GPPS-D03	22484±11677	17771±7724	15241±7198	14094±6774	13011±6970
GPPS-D05	58470±40474	50843±35892	38687±28898	35286±26143	32864±24726
GPPS-D06	55014±13242	47782±11428	36344±10521	33690±10009	30572±8824
GPPS-D14	71311±31278	62090±27322	44263±22117	40646±20795	37835±18810
HDPE-D01	16605±8660	12654±6780	8777±4641	7855±4323	6579±3623
HDPE-D02	15178±6048	10817±3722	7729±2835	7113±2260	5335±2150
HDPE-D03	97495±60048	83943±53418	65693±42727	61092±39384	44896±30119
HDPE-D05	66441±39487	57807±35010	41815±25715	39007±24066	28171±17283
HDPE-D06	50593±41970	43309±36585	32373±30848	30250±28976	23149±23382
HDPE-D14	68178±36726	59617±33702	48677±28923	45606±27396	36571±21769
HIPS-D01	34797±19834	29208±17216	18060±12828	16870±12035	14043±10337
HIPS-D02	17390±8435	14418±7310	10542±6468	9502±5962	8728±5739
HIPS-D03	23653±18351	20203±15972	17212±14236	16129±13358	15447±12794
HIPS-D05	31914±18755	27711±16686	19889±14479	18591±13406	17258±13052
HIPS-D06	96205±7056	85153±5861	68748±5456	58582±7669	54613±7100
HIPS-D14	27286±10906	23758±9742	17489±7488	14443±6129	13990±5945
LDPE-D01	50907±37880	44320±33155	37044±29964	35977±29217	28257±25777
LDPE-D02	18393±17206	13114±11501	8331±7028	7106±5490	4112±1927
LDPE-D03	51387±20293	44478±18521	38830±17425	33520±13129	28583±14829
LDPE-D05	45989±56653	19420±20720	14787±16486	11351±11519	5043±1865
LDPE-D06	21473±5780	16840±5451	12116±3933	11377±3680	8867±3243
LDPE-D14	71655±44581	61148±39396	48346±32656	44855±30677	41267±29279
PP-D01	51573±39834	44402±35166	36970±30582	35337±29646	27811±22361
PP-D02	8193±3357	6119±2666	4290±2094	3966±2002	3438±1837
PP-D03	23446±28260	19115±23898	15240±21089	14649±20377	11247±15968
PP-D05	38427±19436	30271±16411	20466±11969	19336±11423	15086±9149
PP-D06	63783±55543	55850±49890	48901±46660	46523±44786	39554±38537
SW-FL-D01	71005±22604	62451±19708	54987±16575	52086±15113	42394±12608
SW-FL-D02	87805±26463	78287±24287	69289±21455	64415±18044	47259±10196
SW-FL-D03	125427±28856	109642±25014	96005±22683	87755±22359	75028±19235
SW-FL-D05	69809±23570	61436±28568	53489±25746	50665±24250	43924±20640
SW-FL-D06	70293±31788	61436±28568	53489±25746	50665±24250	43924±20640
SW-FL-D14	55144±18401	47992±17007	39960±15314	35331±13543	32449±12841
SW-PA-D01	25189±10565	21420±8987	16524±6980	14968±6515	9574±4716
SW-PA-D02	77682±61098	67762±55122	54946±47406	48187±41391	27138±21537
SW-PA-D03	41727±16994	35648±15144	27377±11732	24376±10084	14196±5671
SW-PA-D05	109115±61693	96505±55426	79147±47043	71034±41225	46723±33846
SW-PA-D06	58880±41377	50474±36166	37321±27134	34850±25043	19287±12851
SW-PA-D14	79269±34263	68284±29993	54665±24055	51237±23020	36832±16324
Total reads	6291476	5356510	4289160	3933915	3144622

High-Quality reads: 3,144,622

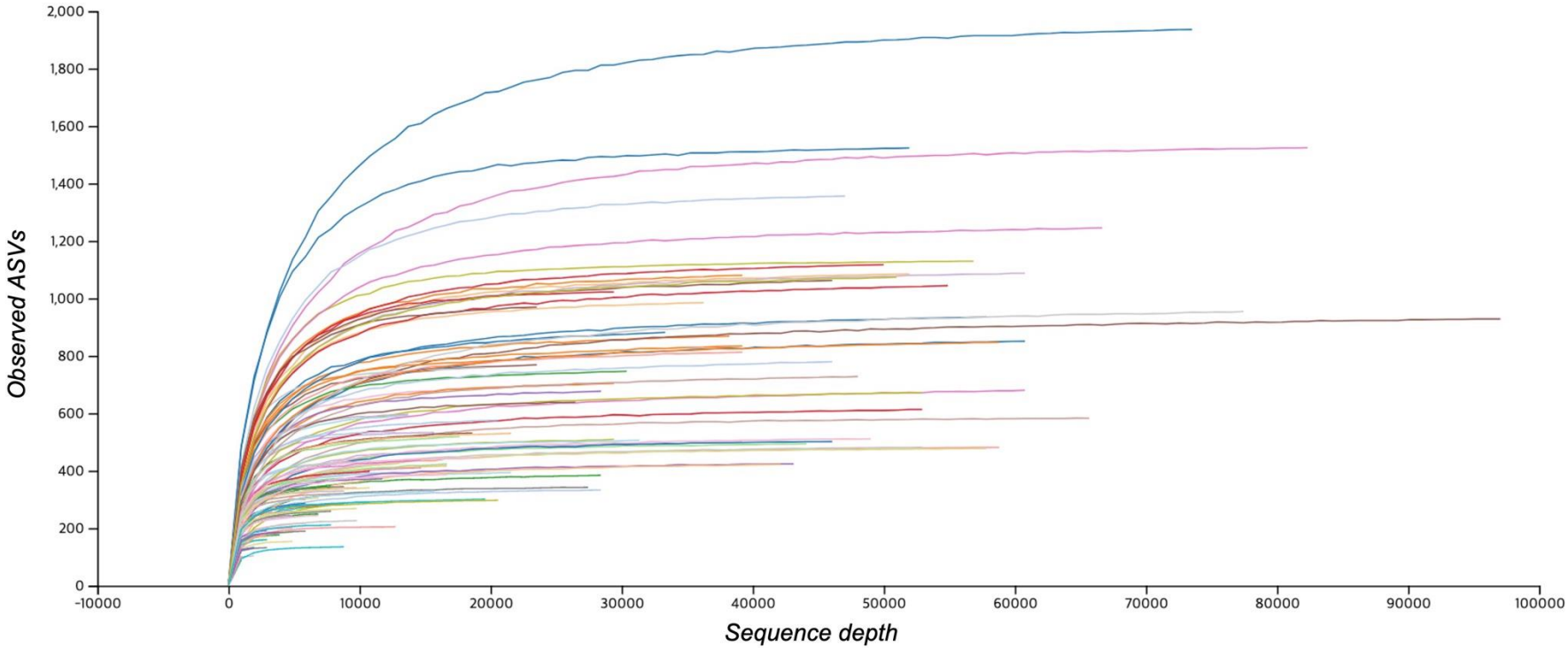

Figure 5. Rarefaction curves for observed ASVs per 122 samples.

3.2.2. Alpha Diversity

Alpha diversity indices (Chao1, Inverse Simpson, Shannon, and ACE) were calculated to assess diversity of prokaryotic communities. Results revealed a range of values for microplastic samples: Chao1 (93–1987), Inverse Simpson (4.53–195.37), Shannon (3.23–6.36), and ACE (93.56–1959.42). In comparison, bulk seawater samples exhibited the following ranges: Chao1 (188–1127), Inverse Simpson (7.96–98.91), Shannon (3.35–5.69), and ACE (187.4–1100.7) (Table 3). The variation of the microplastic samples was higher than bulk seawater samples. In addition, the value of microplastic samples initially decreased and then tended to increase again (Figure 6). The highest alpha diversity indices showed in HDPE at Day 3. However, all alpha diversity indices did not show significantly differences among the groups and the exposure time ($p>0.05$).

Table 3. Summary of alpha diversity indices (Mean±SD) including Chao1, InvSimpson, Shannon, ACE. (SW; Seawater, FL; Free-living fraction, PA; Particle-attached fraction, MP; Microplastics)

Sample Name	Chao1	Inverse Simpson	Shannon	ACE
SW-FL-D01	524±123	62.66±5.35	4.92±0.13	507.06±116.86
SW-FL-D02	500±57	48.01±16.7	4.72±0.22	478.35±41.77
SW-FL-D03	772±188	62.2±11.39	5.01±0.22	746.05±182.42
SW-FL-D05	458±94	48.59±3.57	4.67±0.1	452.27±93.48
SW-FL-D06	499±193	46.11±16.37	4.71±0.35	491.19±189.43
SW-FL-D14	424±87	48.74±9.96	4.71±0.22	415.98±86.68
SW-PA-D01	269±124	44.14±42.06	4.34±0.93	266.35±120.74
SW-PA-D02	556±270	64.78±15.32	5.03±0.2	544.38±262.72
SW-PA-D03	398±118	61.12±7.99	4.9±0.2	387.59±108.78
SW-PA-D05	793±454	60.54±28.11	5.04±0.52	779.8±443.8
SW-PA-D06	543±335	56.11±34.64	5.01±0.61	532.65±325.51
SW-PA-D14	815±365	85.84±20.41	5.39±0.42	797.82±354.89
MP-GPPS-D01	274±44	75.22±26.19	4.94±0.19	273.47±42.83
MP-GPPS-D02	261±145	31.19±5.49	4.26±0.28	259.54±143.72
MP-GPPS-D03	238±85	23.05±18.33	3.86±0.74	234.9±86.47
MP-GPPS-D05	612±270	42.42±48.9	4.67±0.71	596.61±267.6
MP-GPPS-D06	733±167	75.09±28.8	5.39±0.25	716.24±160.04
MP-GPPS-D14	823±272	98.22±25.96	5.51±0.2	808.13±268.16
MP-HDPE-D01	267±157	70.68±31.92	4.75±0.52	264.32±155.74
MP-HDPE-D02	201±73	55.25±25.03	4.53±0.4	200.81±72.22
MP-HDPE-D03	1328±688	148.25±25.51	5.98±0.36	1311.16±678.98
MP-HDPE-D05	825±414	120.27±19.9	5.65±0.39	814.14±406.6
MP-HDPE-D06	626±446	87.18±40.08	5.3±0.47	619.92±444.01
MP-HDPE-D14	791±292	65.94±4.27	5.32±0.18	777.8±289.65
MP-HIPS-D01	599±393	119.75±43.47	5.45±0.63	594.83±391.72
MP-HIPS-D02	288±121	45.87±7.96	4.6±0.1	283.64±119.71
MP-HIPS-D03	317±182	24.04±3.86	4.21±0.2	313.33±178.56
MP-HIPS-D05	361±154	23.46±20.81	4.34±0.54	356.81±149.27
MP-HIPS-D06	886±77	57.75±20.87	5.28±0.13	871.64±79.4
MP-HIPS-D14	389±97	54.6±1.64	4.84±0.12	373.78±102.79
MP-LDPE-D01	746±418	91.94±75.38	5.54±0.54	735.93±413.79
MP-LDPE-D02	212±85	36.64±3.39	4.48±0.21	209.54±80.04
MP-LDPE-D03	570±141	42.37±51.36	4.51±0.94	560.59±142.28
MP-LDPE-D05	208±63	24.61±2.81	4.3±0.24	207.02±62.81
MP-LDPE-D06	304±88	37.49±10.68	4.65±0.07	302.93±89.19
MP-LDPE-D14	916±516	129.23±37.3	5.65±0.5	889.89±498.61
MP-PP-D01	939±572	111.12±73.36	5.73±0.56	917.35±562.78
MP-PP-D02	156±56	27.44±22.18	3.91±0.65	153.04±52.41
MP-PP-D03	429±539	48.4±11.86	4.72±0.83	421.59±526.02
MP-PP-D05	532±263	74.73±14	5.28±0.35	526.7±258.94
MP-PP-D06	880±628	68.48±2.9	5.36±0.35	864.24±610.57

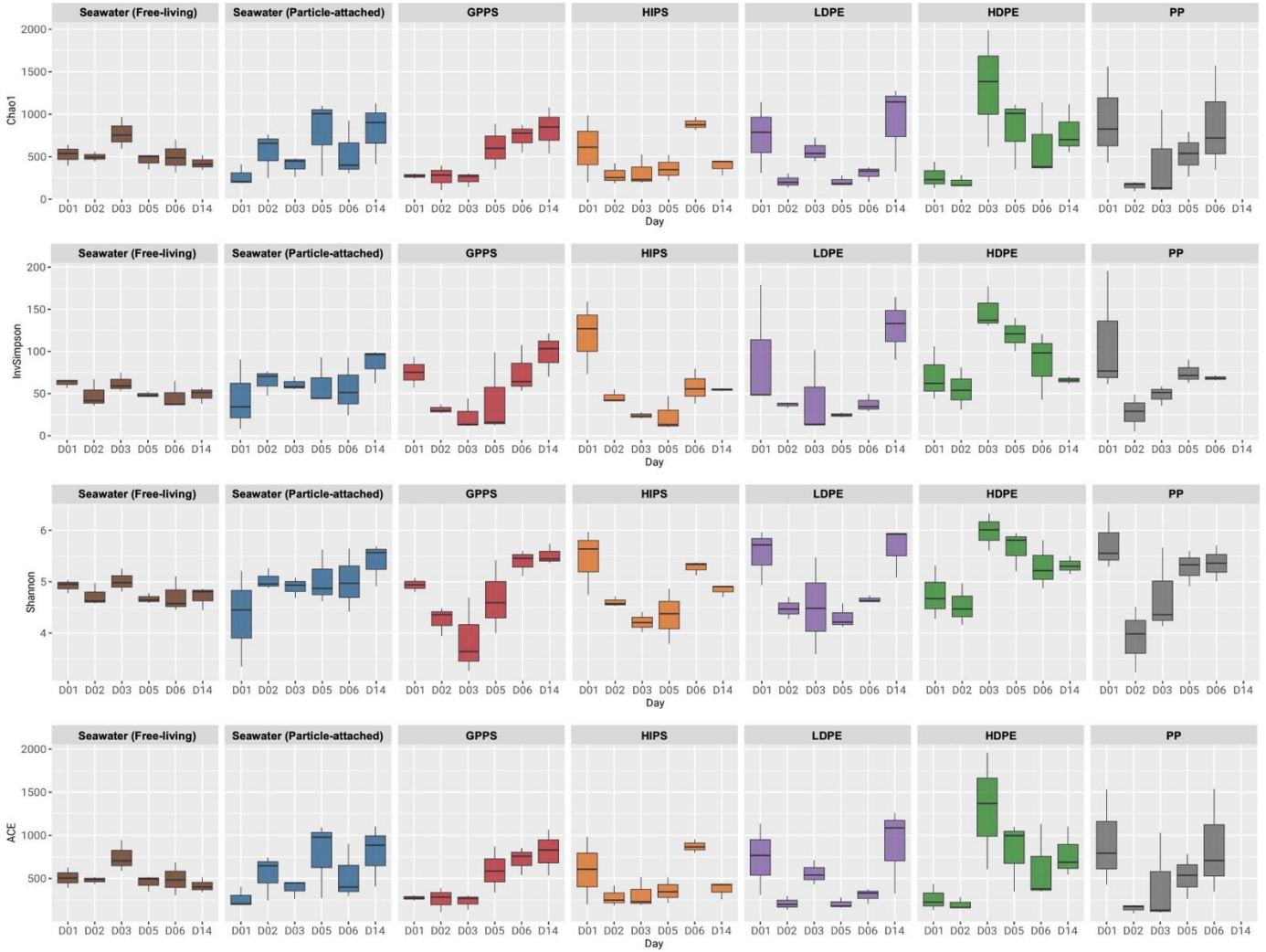

Figure 6. Alpha diversity indices (Chao1, Inverse Simpson, Shannon, and ACE) across the groups.

3.2.3. Beta Diversity

Principal Coordinates Analysis (PCoA) plots based on Bray-Curtis dissimilarities revealed significant differences between microplastic and bulk seawater prokaryotic communities (Figure 7a). Specifically, at Day 14, the microplastic prokaryotic communities exhibited the highest dissimilarity distance from bulk seawater communities (Figure 7b and Figure 8). In addition, the dissimilarity distance of prokaryotic communities among the different polymer types showed the most significant decrease at Day 14 (Figure 8). Notably, the particle–attached communities were included in microplastic communities at Day 1 and Day 2. Furthermore, the free–living prokaryotic communities were observed to be more stable variation than other communities.

The Analysis of similarity (ANOSIM) analysis based on Bray-Curtis dissimilarities confirmed the clear distinction between microplastic and bulk seawater communities from Day 5 to Day 14 (R=0.938–1.000, p=0.001). The lowest R value was 0.400 at Day 1 and p-value was 0.002. The results of pairwise ANOSIM analysis showed comparisons of prokaryotic communities based on both groups and exposure time, as indicated in Table 4. All communities of polymer types were distinguished from seawater communities. Moreover, the influence of these factors was observed across all samples, encompassing microplastic and bulk seawater samples (Global ANOSIM, R=0.525, p=0.001 for groups and R=0.152, p=0.001 for exposure time). Furthermore, the communities across the exposure time did not showed differences among the exposure time. To conduct a more detailed analysis on the microplastic communities, ANOSIM pairwise analysis was performed on the

microplastic communities, excluding the bulk seawater communities (Table 5). The results obtained from the comparisons of the different polymer types did not reveal significant differences, as indicated by the ANOSIM analysis based on Bray-Curtis dissimilarity (Table 5) and based on unweighted Unifrac distance (data not shown), and PCoA plots. Additionally, the microplastic communities across the exposure time factor were observed to be similar communities of Day 2 and Day 3, as well as Day 5 and Day 6 ($R=0.034–0.045$, $p>0.05$) (Table 5). However, Day 14 communities were differentiated from other exposure time points ($R=0.584–0.848$, $p=0.001$)

In summary, alpha diversity of microplastic and bulk seawater prokaryotic communities did not show significantly differences among the groups and the exposure time. However, microplastic-associated prokaryotic communities were distinct from bulk seawater communities based on Bray-Curtis dissimilarity. Notably, the dissimilarity values were found to be highest at Day 14. In addition to, beta diversity of the microplastic-associated prokaryotic communities influenced by exposure time. Moreover, it was difficult to observe an influence of polymer type on microplastic-associated prokaryotic communities.

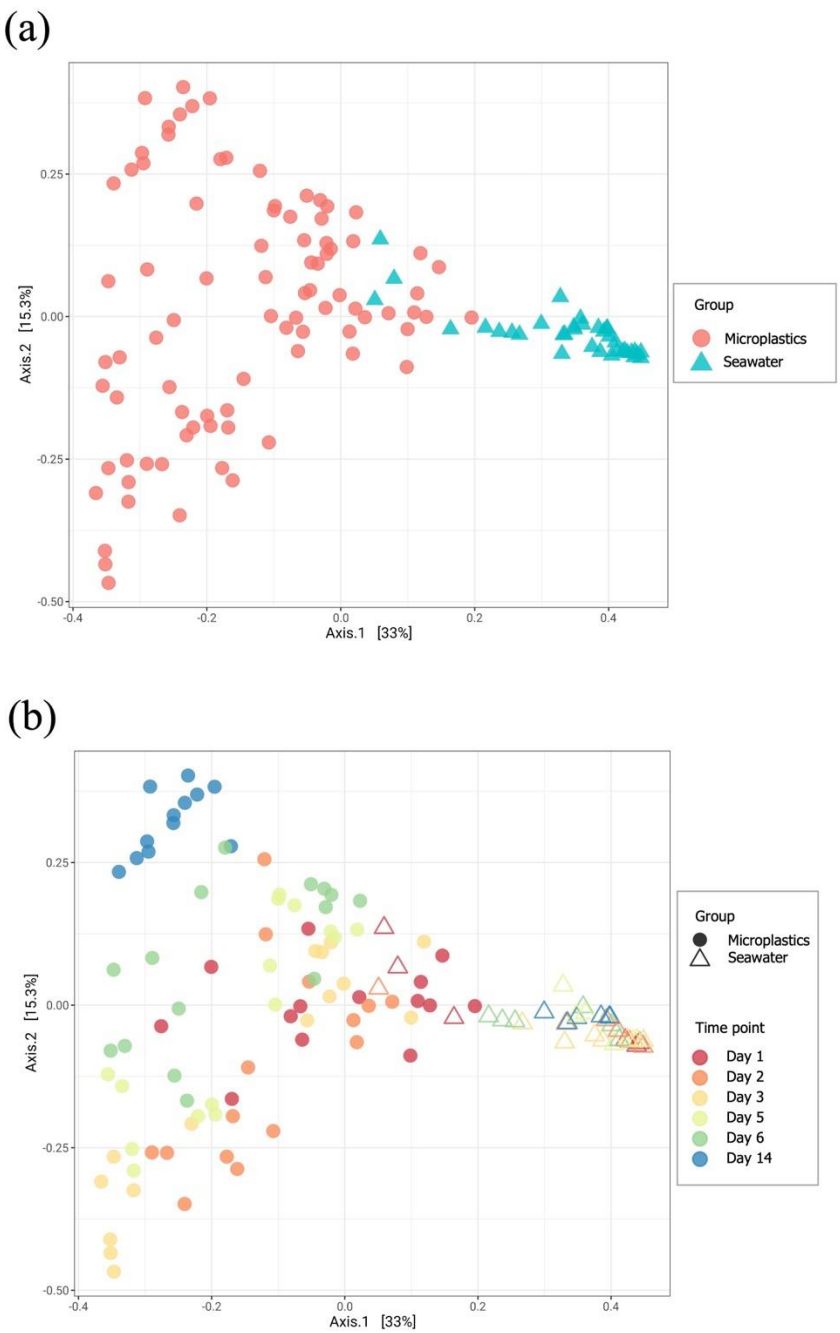

Figure 7. Principal Coordinate Analysis (PCoA) plots based on Bray-Curtis dissimilarity distance grouped by microplastics and seawater (a) and including time point (b).

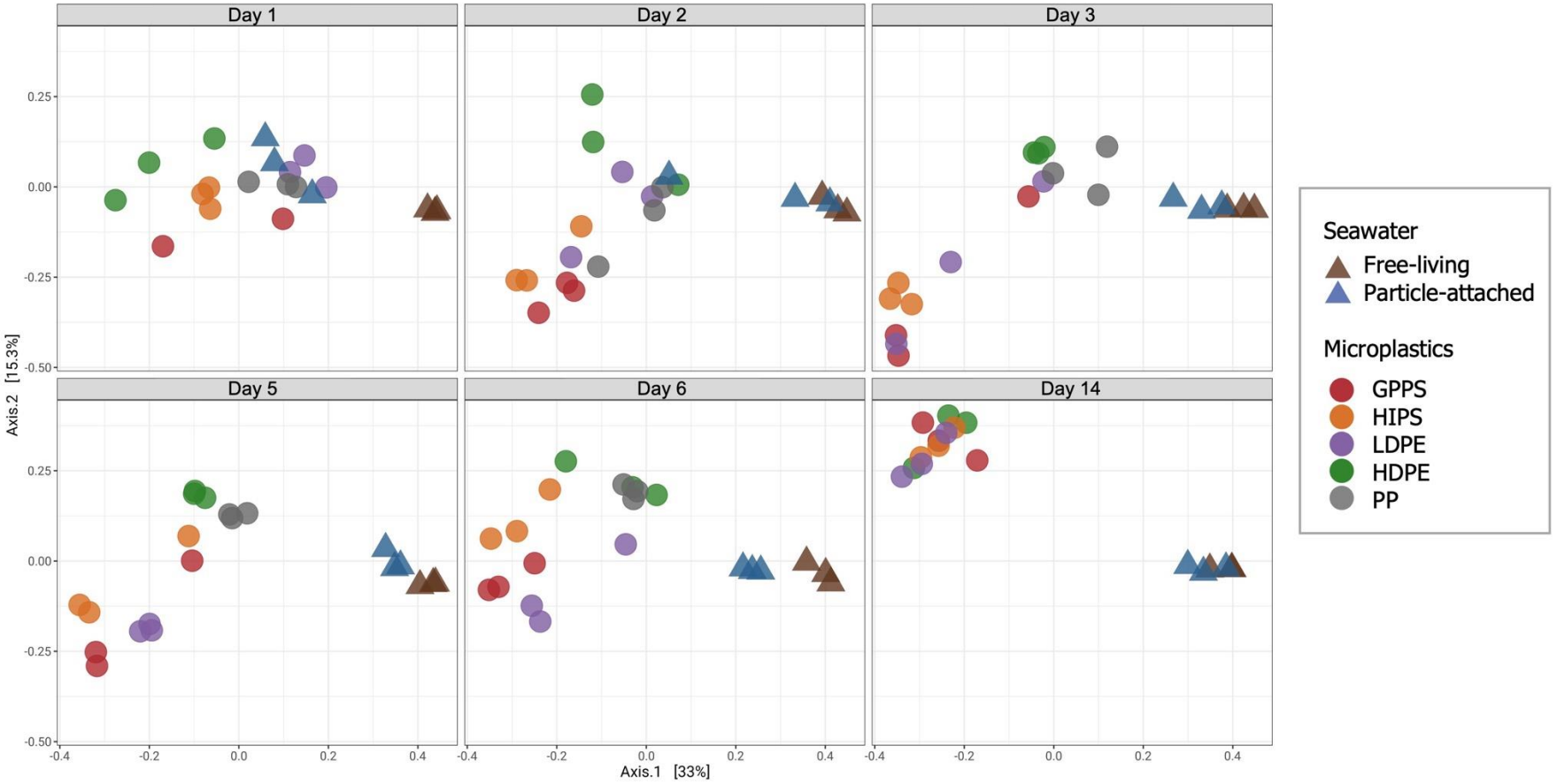

Figure 8. Principal Coordinates Analysis (PCoA) plots based on Bray-Curtis dissimilarity distance among the groups of prokaryotic communities.

Table 4. Analysis of similarity (ANOSIM) pairwise analysis based on Bray-Curtis dissimilarities among the groups (microplastics and seawater fraction) and exposure time points.

Microplastics and seawater community		
Factor	R	P value
Group		
Global ANOSIM	**0.525**	**0.001**
GPPS / HDPE	0.318	0.001
GPPS / HIPS	0.064	0.066
GPPS / LDPE	0.146	0.006
GPPS / PP	0.457	0.001
GPPS / FL	0.896	0.001
GPPS / PA	0.690	0.001
HDPE / HIPS	0.334	0.001
HDPE / LDPE	0.201	0.001
HDPE / PP	0.258	0.001
HDPE / FL	0.833	0.001
HDPE / PA	0.572	0.001
HIPS / LDPE	0.275	0.001
HIPS / PP	0.517	0.001
HIPS / FL	0.962	0.001
HIPS / PA	0.754	0.001
LDPE / PP	0.176	0.002
LDPE / FL	0.797	0.001
LDPE / PA	0.565	0.001
PP / 0.2	0.945	0.001
PP / PA	0.602	0.001
FL / PA	0.201	0.001
Exposure time		
Global ANOSIM	**0.152**	**0.001**
Day 1 / Day 2	0.050	0.068
Day 1 / Day 3	0.052	0.074
Day 1 / Day 5	0.121	0.010
Day 1 / Day 6	0.193	0.002
Day 1 / Day 14	0.302	0.001
Day 2 / Day 3	-0.014	0.579
Day 2 / Day 5	0.079	0.033
Day 2 / Day 6	0.179	0.004
Day 2 / Day 14	0.337	0.001
Day 3 / Day 5	0.031	0.155
Day 3 / Day 6	0.114	0.013
Day 3 / Day 14	0.335	0.001
Day 5 / Day 6	0.024	0.168
Day 5 / Day 14	0.285	0.001
Day 6 / Day 14	0.163	0.014

Table 5. Analysis of similarity (ANOSIM) pairwise analysis based on Bray-Curtis dissimilarities among polymer types and exposure time points.

Microplastic (excluding seawater community)		
Factor	R	P value
Polymer types		
Global ANOSIM	**0.267**	**0.001**
GPPS / HDPE	0.318	0.001
GPPS / HIPS	0.064	0.072
GPPS / LDPE	0.146	0.004
GPPS / PP	0.457	0.001
HDPE / HIPS	0.334	0.001
HDPE / LDPE	0.201	0.001
HDPE / PP	0.258	0.001
HIPS / LDPE	0.275	0.001
HIPS / PP	0.517	0.001
LDPE / PP	0.176	0.003
Exposure time		
Global ANOSIM	**0.378**	**0.001**
Day 1 / Day 2	0.169	0.003
Day 1 / Day 3	0.192	0.004
Day 1 / Day 5	0.303	0.001
Day 1 / Day 6	0.451	0.001
Day 1 / Day 14	0.848	0.001
Day 2 / Day 3	0.045	0.110
Day 2 / Day 5	0.204	0.003
Day 2 / Day 6	0.386	0.001
Day 2 / Day 14	0.818	0.001
Day 3 / Day 5	0.116	0.044
Day 3 / Day 6	0.271	0.002
Day 3 / Day 14	0.801	0.001
Day 5 / Day 6	0.034	0.192
Day 5 / Day 14	0.851	0.001
Day 6 / Day 14	0.584	0.001

3.3. Taxonomic Structure, Major ASVs, Functional Inference, and Correlation with Environmental Parameters

3.3.1. Taxonomic Structure

At the class level, the taxonomic composition was as follows: Bacteroidia accounted for 38.81±14.73 % of the total community, followed by Alphaproteobacteria at 27.45±13.81 %, and Gammaproteobacteria at 22.04±19.97 %. Cyanobacteriia contributed 2.67±2.97 %, while Acidimicrobiia represented 1.79±1.58%. Nitrososphaeria, Planctomycetes, Bacilli, Actinobacteria, and Thermoplasmata accounted for 1.14±1.57 %, 1.06±1.40 %, 0.80±1.64 %, 0.56±1.82 %, and 0.54±0.77 %, respectively. Especially, Thermoplasmata, affiliated with the Archaea domain, exhibited a higher relative composition in seawater communities (1.27±1.0 4%) compared to microplastic communities (0.23±0.29 %).

The dominant taxonomic composition of the merged prokaryotic communities of microplastics and seawater at the order level were Flavobacteriales (33.05±12.42 %), Rhodobacterales (18.18±12.05 %), Oceanospirillales (14.67±19.43 %), SAR11 clade (4.89±6.25 %), Chitinophagales (2.73±3.32 %), Synechococcales (2.37±2.67 %), Vibrionales (1.53±2.03 %), Actinomarinales (1.24±1.52 %), Nitrosopumilales (1.14±1.57 %), and Rhizobiales (1.05±1.51 %) (Figure 9). Oceanospirillales and Vibrionales taxa were in higher abundance in microplastic-associated communities than in seawater communities. Remarkably, distinct differences in the distribution of Oceanospirillales taxa were observed among various polymer types, with HDPE and PP polymer types exhibiting relatively lower proportions compared to other types. Moreover, the PP polymer type

showed a greater prevalence of Vibrionales taxa in comparison to the other plastic types. In contrast, Actinomarinales, SAR11 clade, and Synechococcales taxa were predominant in seawater communities (Figure 9 and Table 6).

In addition to, the major taxonomic composition at the family level was composed of *Flavobacteriaceae* (21.96±9.39 %), *Rhodobacteraceae* (18.27±12.15 %), *Saccharospirillaceae* (10.85±15.88 %), *Cryomorphaceae* (5.22±3.74 %), Clade I (4.45±5.69 %), *Crocinitomicaceae* (3.70±2.32 %), *Oleiphilaceae* (2.72±4.20 %), *Saprospiraceae* (2.47±2.86 %), *Cyanobiaceae* (2.34±2.77 %), and NS9 marine group (1.72±1.89 %) (Figure 10 and Table 7). Moreover, Clade I, *Crocinitomicaceae*, *Cryomorphaceae*, and *Cyanobiaceae* taxa were higher taxonomic compositions compared to microplastic communities. In microplastic-associated communities, *Oleiphilaceae*, *Saccharospirillaceae*, and *Saprospiraceae* taxa were higher abundance compared to seawater communities. Particularly, the abundance of *Oleiphilaceae* taxa was higher in HIPS and GPPS compared to other polymer types.

These major taxonomic compositions were compared by microplastics and seawater groups at the order and family taxonomic levels (Figure 11). The relative abundance of Chitinophagales, Oceanospirillales, Rhizobiales, and Vibrionales taxa was found to be significantly higher in microplastic communities compared to seawater communities (Figure 11a). Conversely, Actinomarinales, Flavobacteriales, Nitrosopumilales, SAR11 clade, and Synechococcales taxa exhibited significantly higher relative abundance in seawater communities compared to microplastic communities. Although Rhodobacterales taxa showed higher relative abundance in seawater communities, the difference was not statistically significant. At the family

level, *Oleiphilaceae*, *Saccharospirillaceae*, and *Saprospiraceae* taxa showed significantly higher relative abundance in microplastic than seawater communities (Figure 11b). On the other hand, Clade I, *Cryomorphaceae*, *Cyanobiaceae*, and NS9 marine group taxa were significantly more abundant than other taxa in seawater communities. However, no statistically significant differences were observed for *Crocinitomicaceae, Flavobacteriaceae*, and *Rhodobacteraceae* taxa.

To investigate temporal variations within major taxonomic groups in the microplastic communities, a temporal analysis of each major taxonomic group was conducted (Figure 12). At the order level, an increasing trend in the relative abundance of Rhizobiales and Rhodobacterales was observed over time, while Oceanospirillales and Vibrionales exhibited a decreasing trend. Regarding the family level, *Saccharospirillaceae* and *Oleiphilaceae* displayed an initial increase followed by a subsequent decrease within the microplastic communities. Conversely, *Saprospiraceae* and *Rhodobacteraceae* demonstrated a consistent increase in relative abundance over time.

In summary, significant differences were observed in the composition of major taxa between the microplastic community and bulk seawater community at both the order and family levels. Furthermore, distinct variations in community composition were observed within the groups for specific major taxa. Additionally, temporal dynamics were detected within major taxonomic groups in the microplastic community, highlighting the influence of exposure time on their relative abundances.

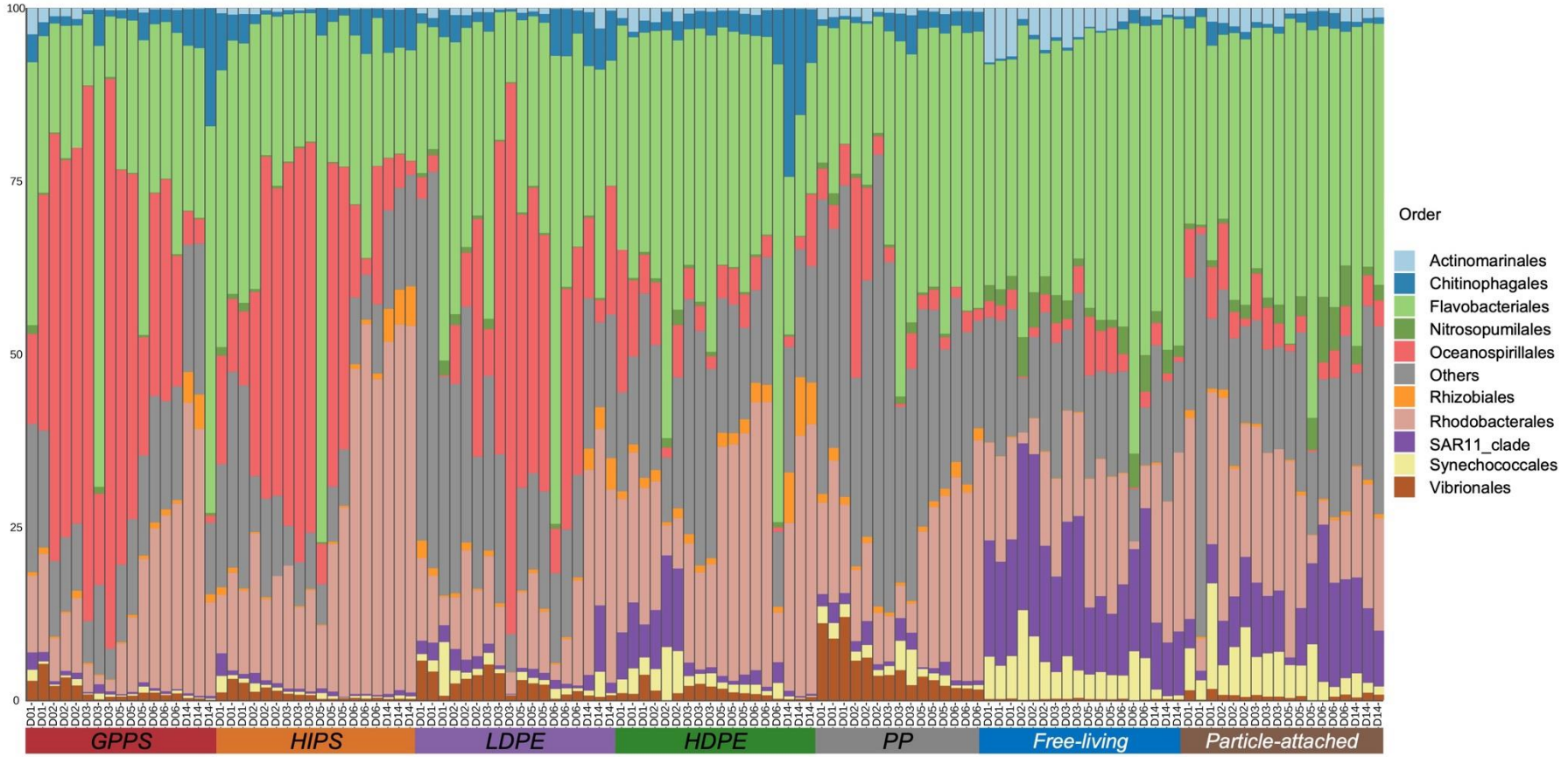

Figure 9. Prokaryotic taxonomic compositions at the order level. Top 10 taxa with the highest abundances were plotted and the other taxa were classified as "Others".

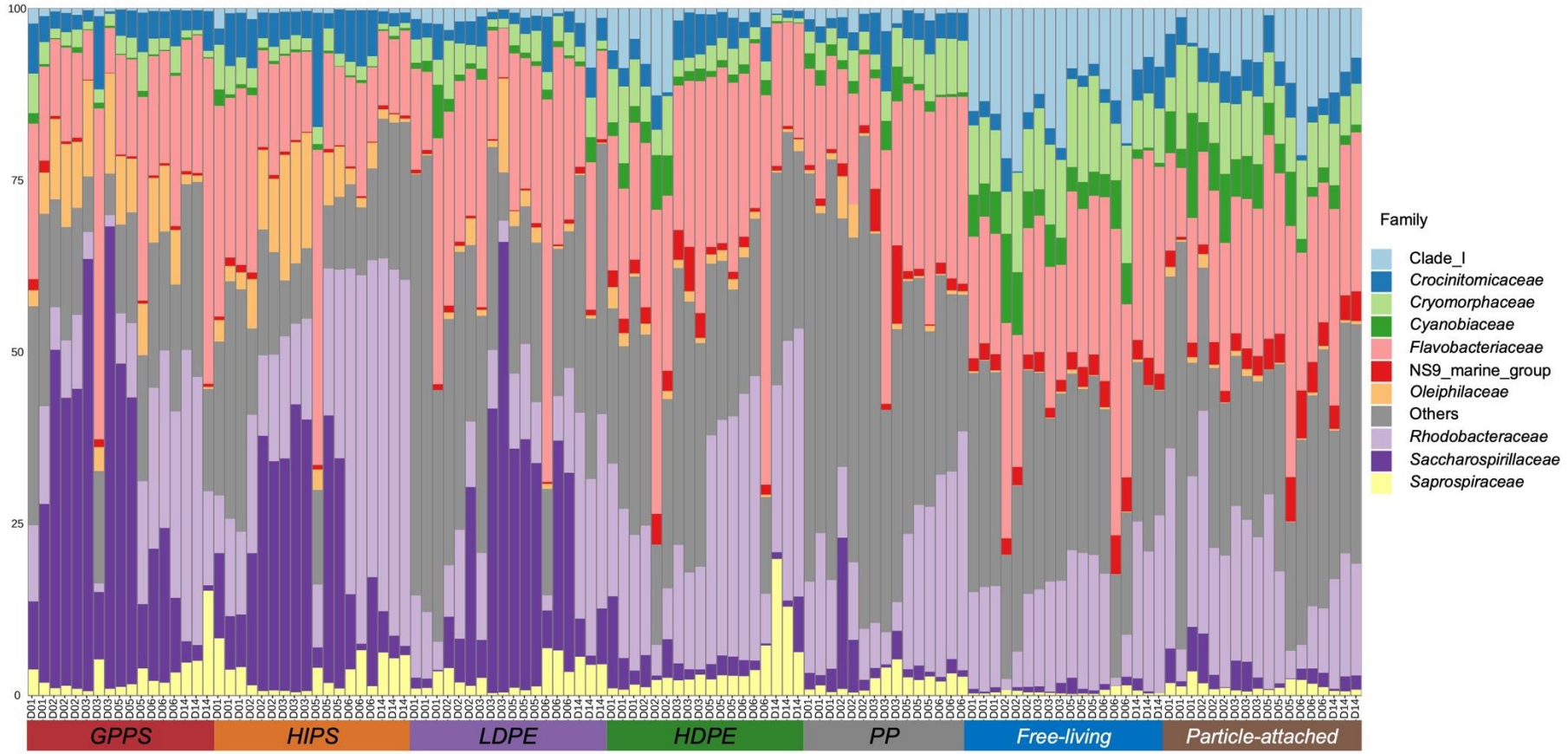

Figure 10. Prokaryotic taxonomic compositions at the family level. Top 10 taxa with the highest abundances were plotted and the other taxa were classified as "Others"

Table 6. Relative abundance (%) of dominant taxa (top 10) at the order taxonomic level among all groups. (Mean±SD)

Order	Microplastics					Seawater	
	GPPS	HIPS	LDPE	HDPE	PP	Free-living	Particle-attached
Actinomarinales	0.73±0.98	0.33±0.32	0.68±0.67	0.89±0.9	0.89±0.47	3.54±2.38	1.56±0.93
Chitinophagales	3.43±3.9	3.16±2.54	3.26±2.59	4.96±5.94	2.22±1.45	0.62±0.47	1.43±0.79
Flavobacteriales	27.38±14.94	27.39±14.06	30.11±13.15	35.7±12.08	32.06±10.7	40.41±7.9	37.79±7.1
Nitrosopumilales	0.29±0.33	0.32±0.37	0.61±0.57	0.51±0.52	0.6±0.5	2.93±1.54	2.6±2.47
Oceanospirillales	35.54±26.02	26.09±20.88	22.96±21.31	5.69±4.8	5.29±7.21	2.82±2.2	3.88±2.63
Rhizobiales	1.03±1.43	1.2±1.85	1.12±1.29	2.45±2.32	1.04±0.54	0.09±0.07	0.43±0.33
Rhodobacterales	15.45±12.06	27.02±17.71	12.4±8.03	23.72±12.07	16.61±9.64	14.43±6.93	17.2±8.48
SAR11 clade	0.65±0.6	0.71±0.71	1.91±2.08	3.8±4.3	1.57±1.05	15.41±5.62	9.39±5.17
Synechococcales	0.43±0.4	0.54±0.53	1.46±1.76	2.11±2	1.75±1.35	4.9±3.01	5.19±3.51
Vibrionales	1.34±1.38	0.88±0.86	2.29±1.71	1.16±0.93	4.74±3.42	0.16±0.08	0.64±0.44

Table 7. Relative abundance (%) of dominant taxa (top 10) at the family taxonomic level among all groups. (Mean±SD)

Family	Microplastics					Seawater	
	GPPS	HIPS	LDPE	HDPE	PP	Free-living	Particle-attached
Clade I	0.58±0.51	0.66±0.64	1.76±1.87	3.57±4.16	1.44±1.02	13.9±5.07	8.51±4.87
Crocinitomicaceae	4.09±2.39	5.38±3.61	3.02±1.78	3.35±1.92	3.6±1.99	2.62±1.61	3.88±1.53
Cryomorphaceae	2.43±1.51	2.36±1.39	3.37±1.75	3.92±2.95	4.97±2.09	10.69±2.93	8.61±2.4
Cyanobiaceae	0.42±0.37	0.53±0.52	1.44±1.78	2.08±2.04	1.69±1.35	4.9±3.02	5.11±3.55
Flavobacteriaceae	19.78±11.98	17.77±9.28	22.94±11.11	25.91±10.13	21.37±7.72	24.05±6.95	21.7±6.06
NS9 marine group	0.56±0.47	0.49±0.32	0.5±0.27	2.15±1.67	2.04±2.96	2.88±1.09	3.38±1.64
Oleiphilaceae	7.59±4.52	6.59±6.02	1.74±3.15	1.19±0.74	1.18±1.79	0.18±0.15	0.57±0.51
Rhodobacteraceae	15.6±12.23	27.21±17.89	12.48±8.14	23.85±12.1	16.68±9.68	14.44±6.93	17.24±8.51
Saccharospirillaceae	27.53±21.86	19.26±15.34	19.03±18.77	3.2±3.25	3.48±5.45	0.74±0.64	2.4±2.2
Saprospiraceae	3.2±3.46	3.12±2.51	2.78±2.13	4.29±4.84	2.11±1.39	0.5±0.38	1.3±0.77

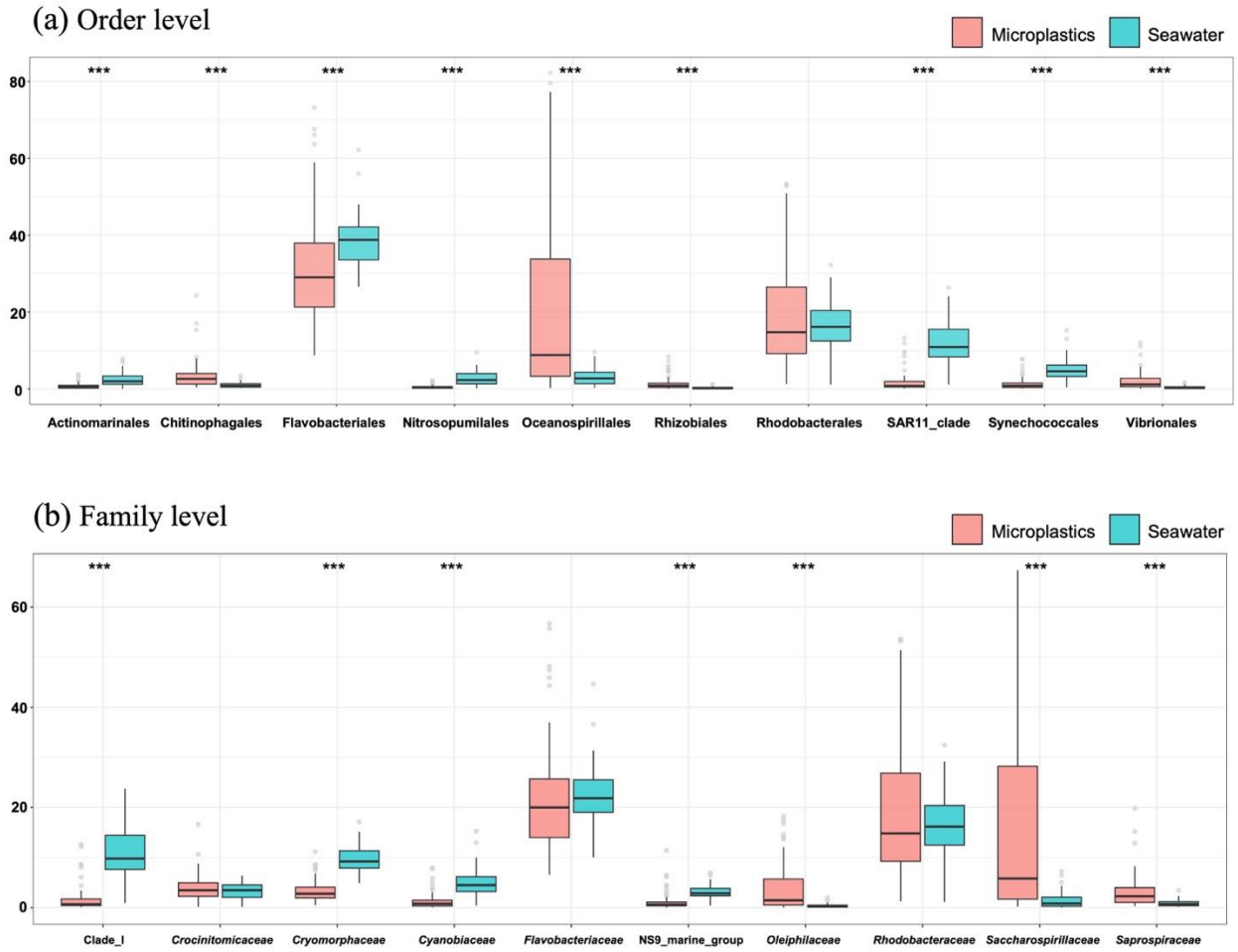

Figure 11. Comparisons of major taxonomic relative abundance among the microplastics and seawater groups at the order level (a) and the family level (b). (*p<0.001)**

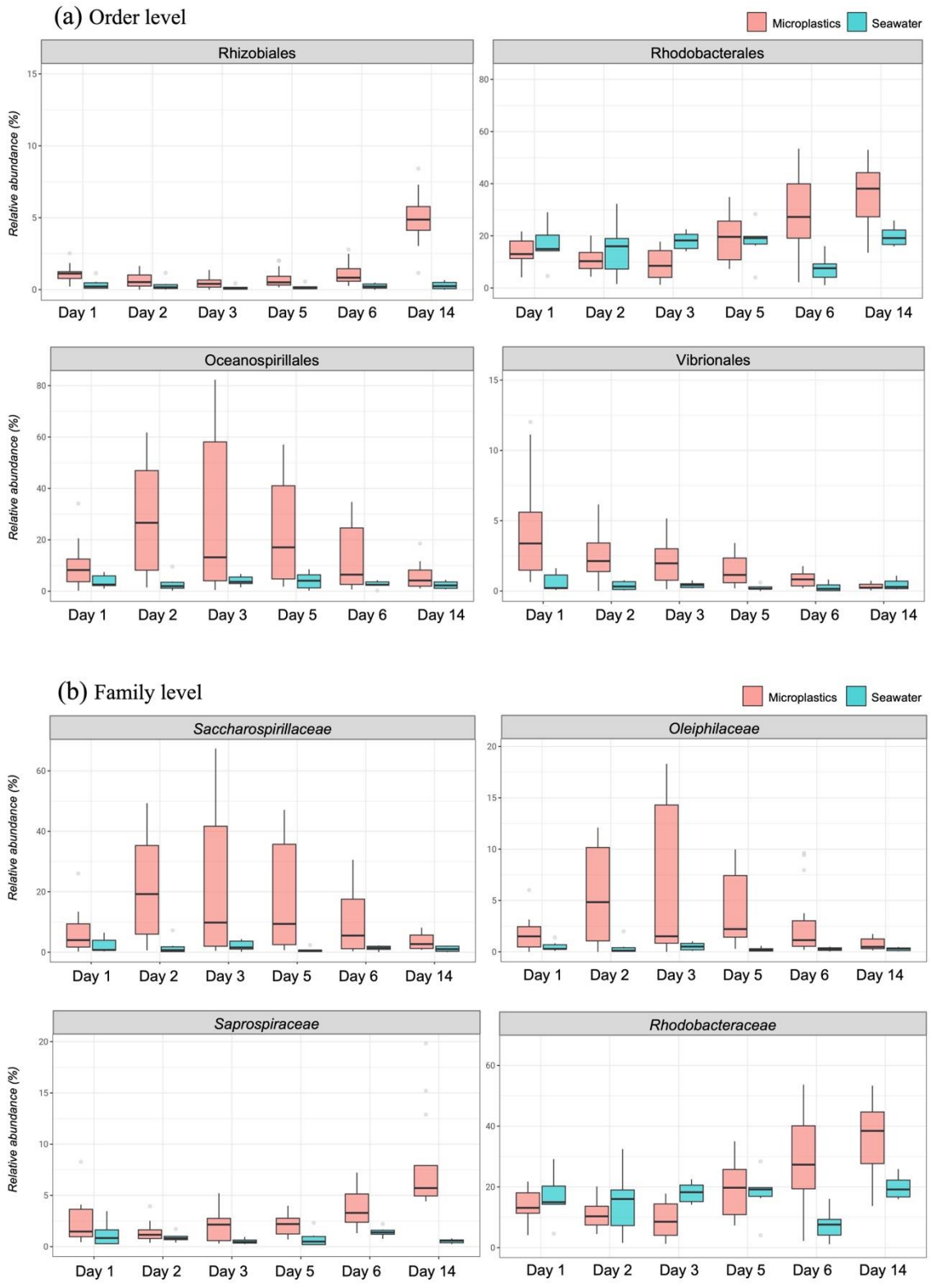

Figure 12. The relative abundance of each major taxa with temporal variations was presented at the order (a) and family (b) levels.

3.3.2. Major ASVs in Microplastic-Associated Prokaryotic Communities

The major ASVs of microplastic-associated prokaryotic communities representing more than 4 % of relative abundance in at least one sample were selected (Figures 13 and 14). The selected ASVs were affiliated with Actinobacteria, Alphaproteobacteria, Bacteroidia, Gammaproteobacteria, Cyanobacteriia, and Clostridia at class level. ASV 7911, ASV 7811, ASV 7795, and ASV 8004 affiliated with *Rhodobacteraceae* increased relative abundance over time (Figure 13). Additionally, ASV 4493, ASV 4471, and ASV 4387 belonging to the *Flavobacteriaceae* also increased relative abundance over time. In contrast, ASV 11670, ASV 11710, ASV 11713, ASV 11715, and ASV 11829, which belong to the *Saccharospirillaceae* family, were observed to be decreased over time.

In addition to, specific taxa showed differences of relative abundance by groups (Figure 14). In the comparison between microplastic-associated communities and bulk seawater communities, notable differences were observed in the relative abundances of selected ASVs. Specifically, ASV3827 affiliated with *Cryomorphaceae* and ASV1984 affiliated with *Cyanobiaceae* were found to be predominant in the bulk seawater community. Additionally, ASVs belonging to Oceanospirillales exhibited a higher overall abundance in the microplastic-associated communities, with minimal variation observed between the particle-attached samples of HDPE and PP. Additionally, ASV 8974, belonging to the genus *Commensalibacter*, exhibited a substantially higher relative abundance in PP samples compared to other polymer types. Additionally, ASV 8534 and ASV 8547, assigned to the SAR11 clade, were specifically detected in LDPE and PP samples, while they were not found in other polymer types.

The LEfSe (Linear Discriminant Analysis Effect Size) analysis revealed the presence of specific taxa within the samples (Figures 15 and 16). Dividing the samples into microplastics and seawater, significant biomarker taxa, such as Gammaproteobacteria, Oceanoshirillales, *Oleibacter*, and *Saccharospirillacea* were observed in microplastic communities (Figure 15). Additionally, the significant biomarker taxa that exhibited differences among the groups were identified at each time point (Figure 16). The results revealed the presence of biomarker taxa for all groups on Day 5 and Day 6. Specifically, HDPE and Free-living samples consistently exhibited

biomarker taxa across all time points. Furthermore, it was observed that the biomarker taxa not only remained consistent within a single polymer type but also shifted between different polymer types.

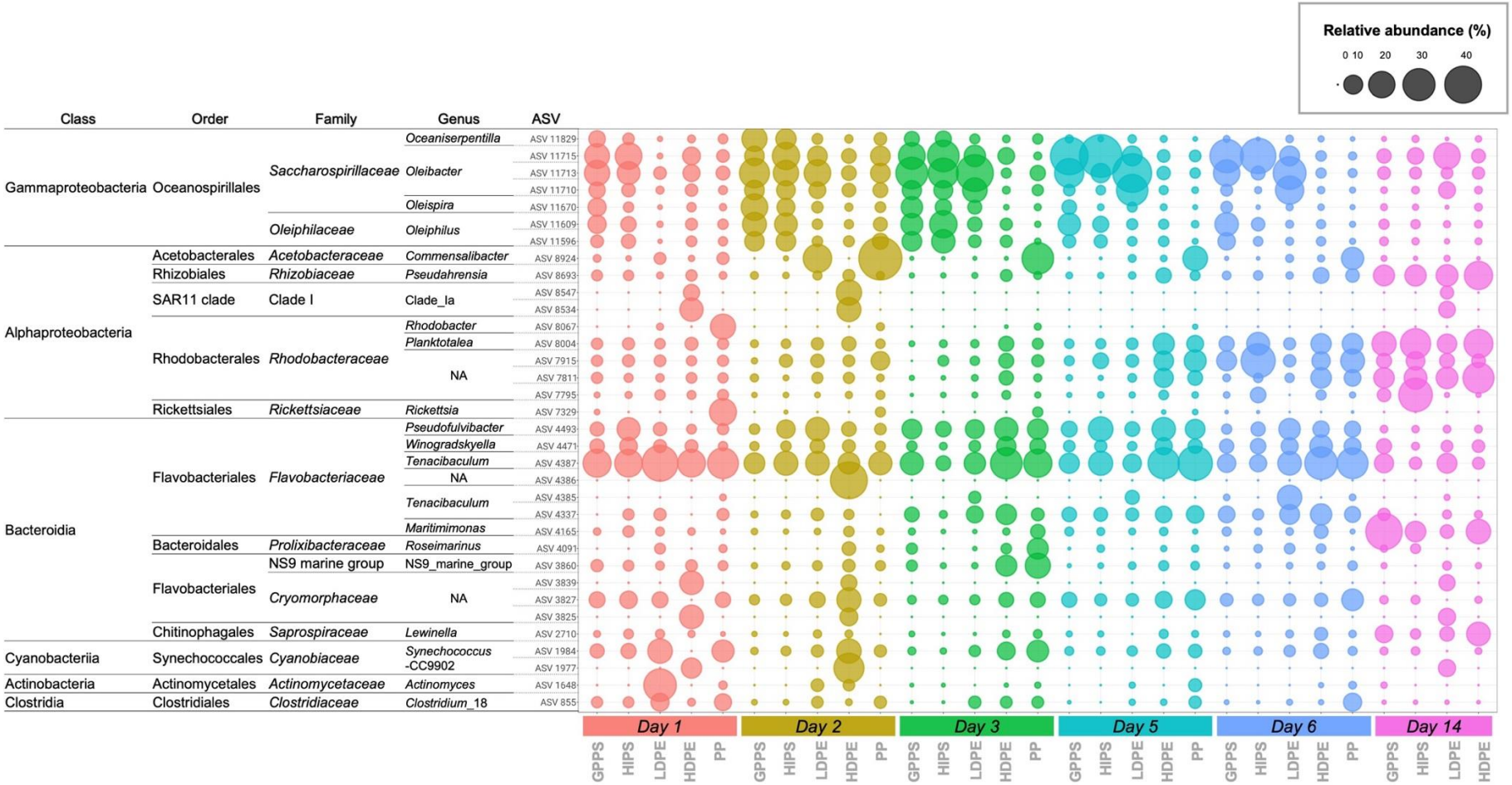

Figure 13. Relative abundance dynamics of major ASVs (>4 %) present in at least one microplastic sample and showing taxonomic affiliation of the ASVs. The color in the bubble plot was specified by the sample across exposure time. NA, not available.

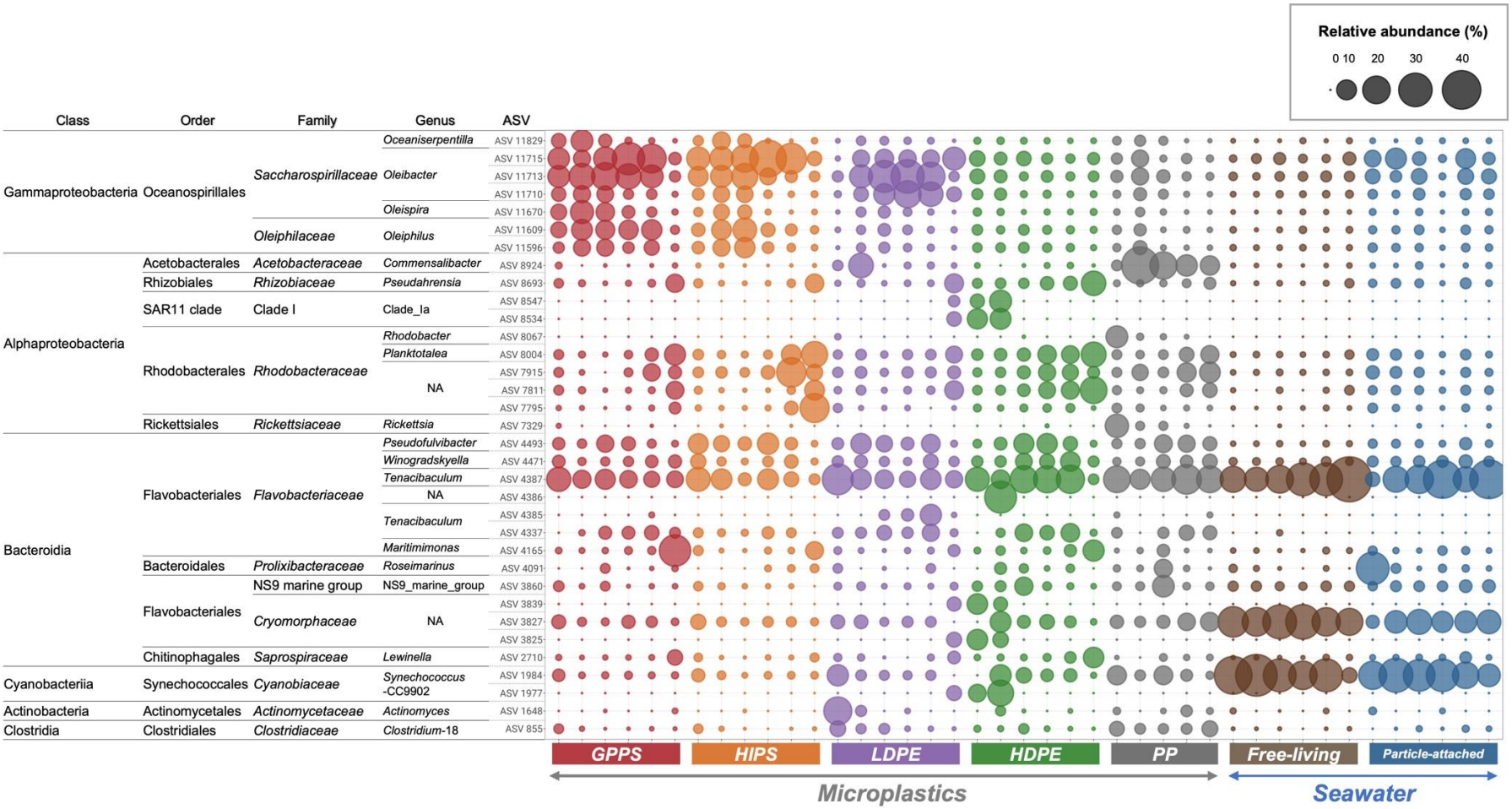

Figure 14. Relative abundance dynamics of major ASVs (>4 %) present in at least one microplastic sample and showing taxonomic affiliation of the ASVs. The color in the bubble plot was specified by the sample across the groups. The seawater communities, including both free-living and particle-attached samples, were included in this analysis to compare them with microplastic communities. NA, not available.

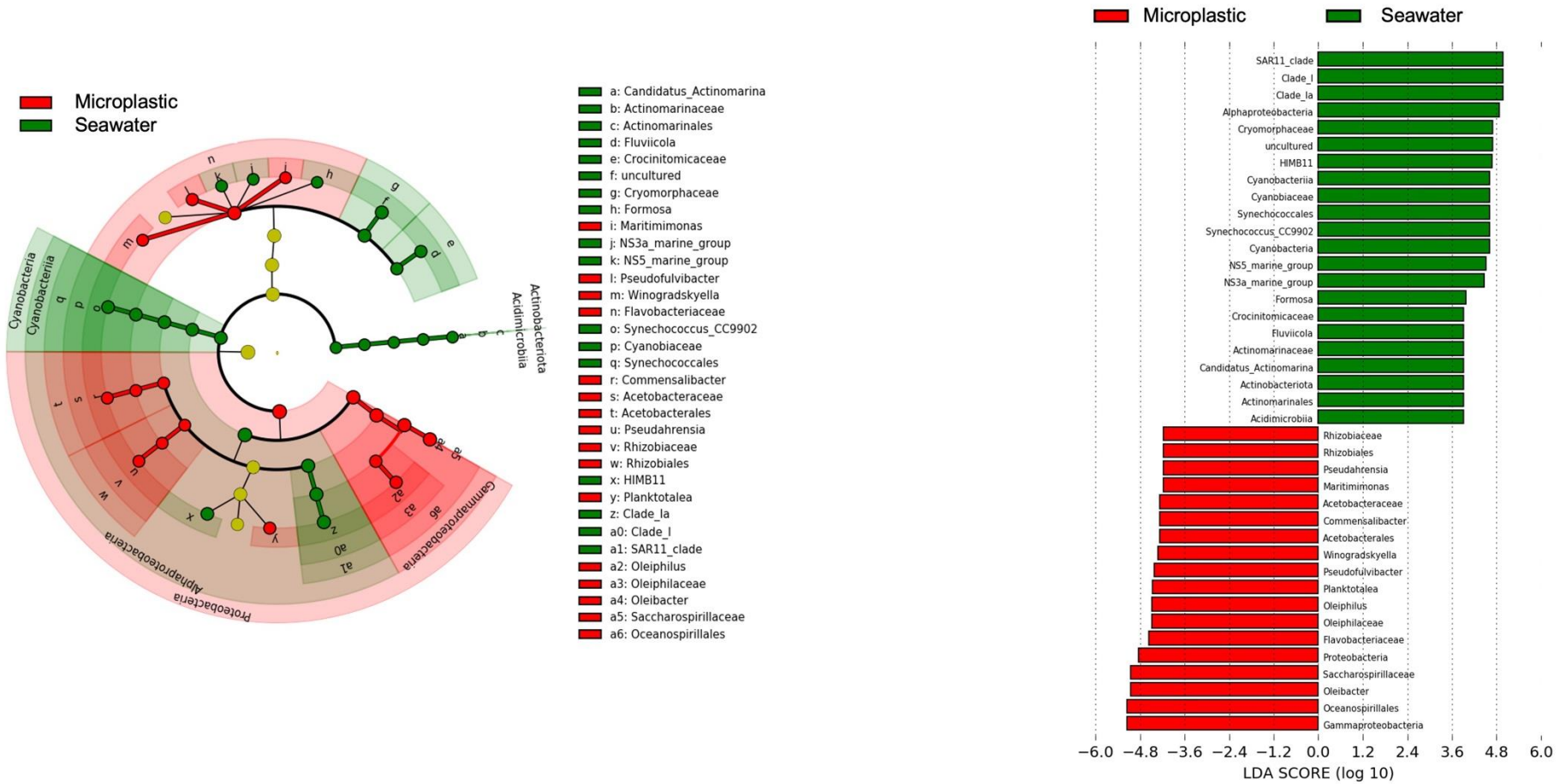

Figure 15. The results of LEfSe (Linear discriminant analysis effect size) analysis across microplastic and seawater samples. Cladogram (left) and LDA (Linear discriminant analysis) score (right).

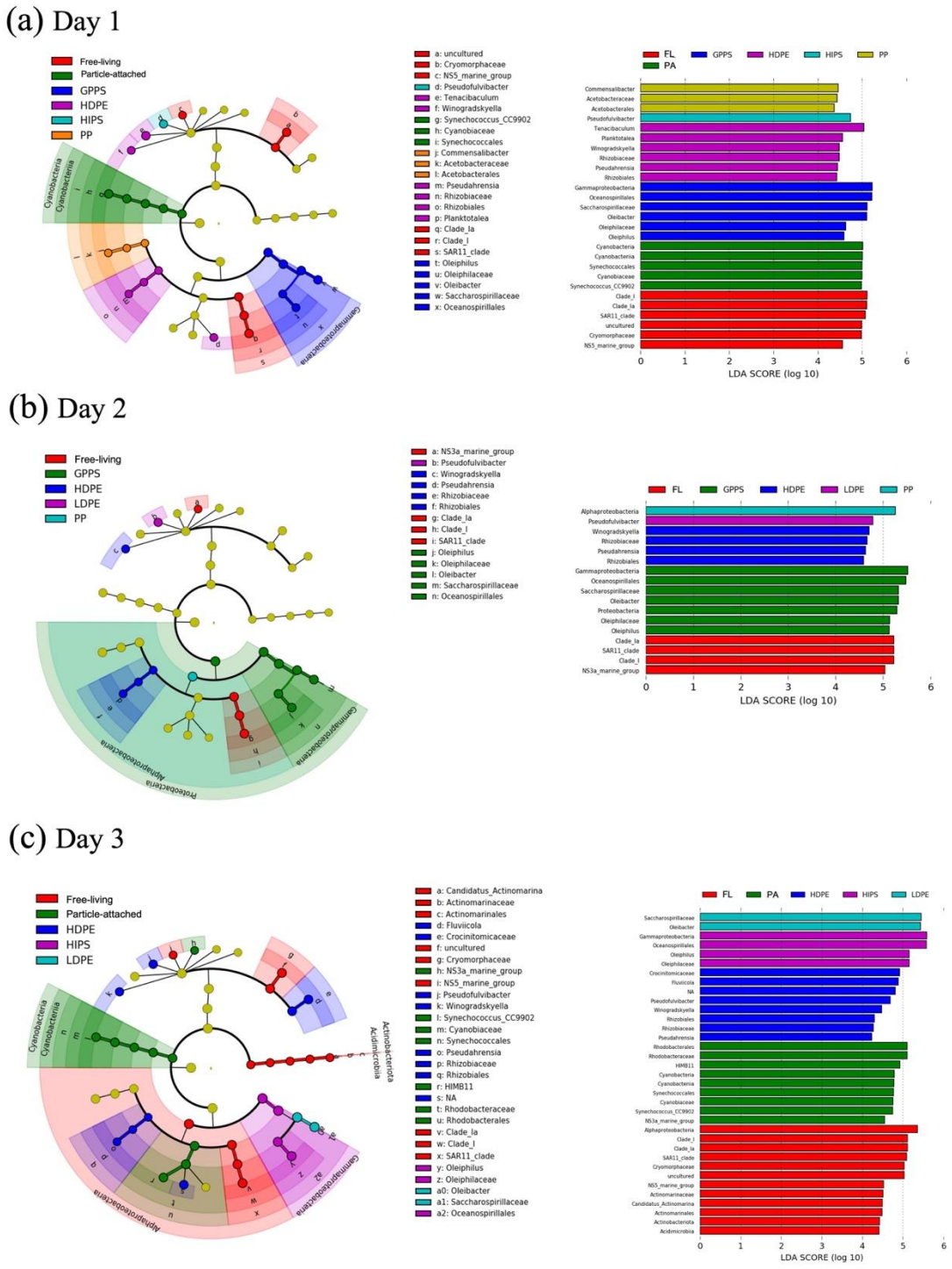

Figure 16. (Continued)

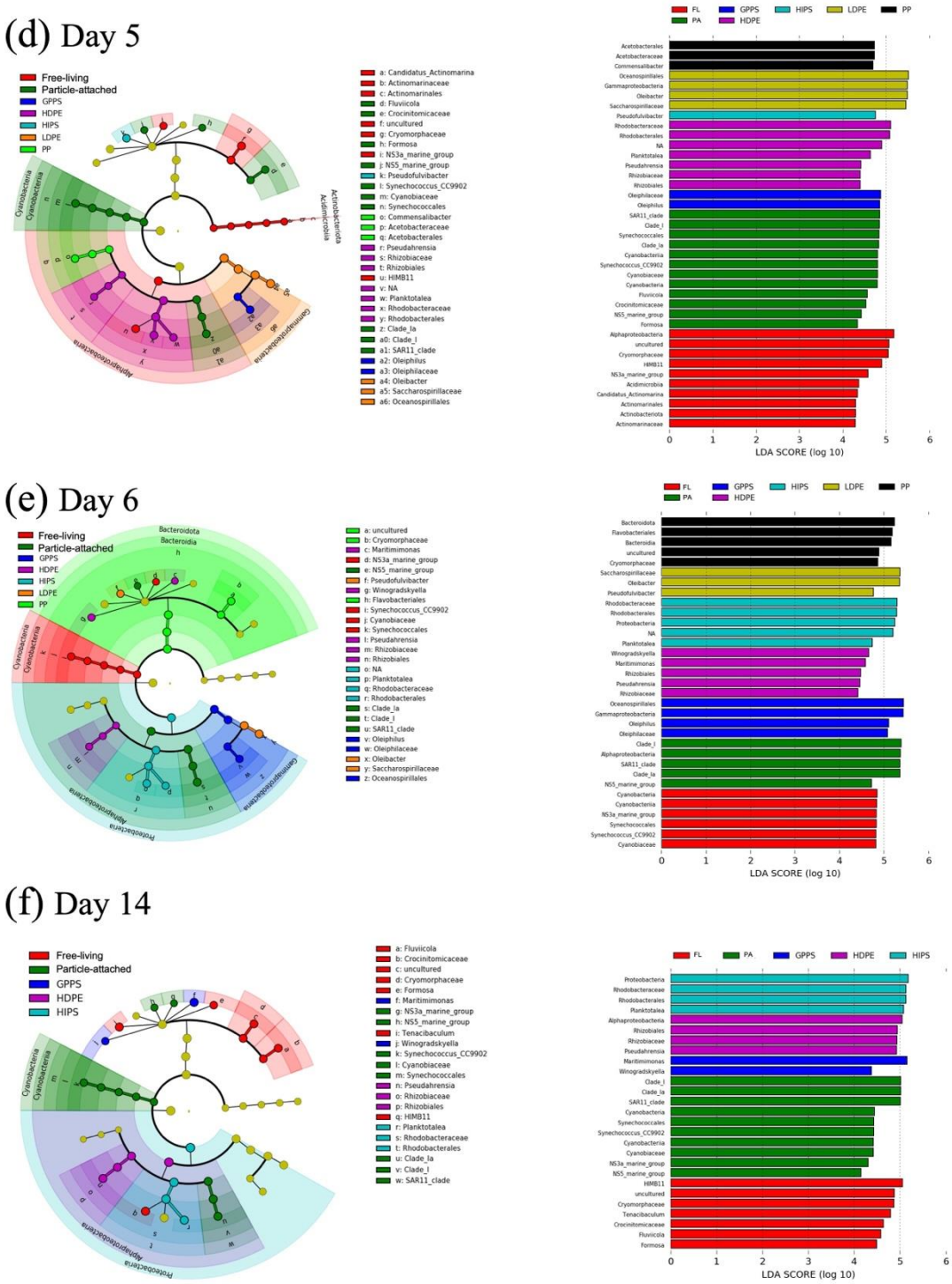

Figure 16. The results of LEfSe (Linear discriminant analysis effect size) analysis across the groups by each time point. Only the groups with statistically significant differences were depicted in the graph, while those without such differences were not shown. Day 1 (a), Day 2 (b), Day 3 (c), Day 5 (d), Day 6 (e), and Day 14 (f). FL, Free-living; PA, Particle-attached.

3.3.3. Functional Inference

The functional profiles of prokaryotic communities were determined by inferring KEGG pathway abundances at level 3 using the PICRUSt2 program. Moreover, NMDS and ANOSIM analyses revealed significant differences in the abundance of KEGG pathways (stress=0.07, R=0.331, p=0.001) between prokaryotic communities associated with microplastics and seawater samples. Additionally, temporal variations were observed in the functions related to benzoate degradation, polycyclic aromatic hydrocarbon degradation, cell motility and secretion, and bacterial motility proteins over time (Figure 17). Notably, microplastic-associated functions of benzoate degradation and polycyclic aromatic hydrocarbon (PAH) degradation represented that microplastic communities exhibited an increase in these functions over time. In contrast, the relative abundance of functions associated with cell motility and secretion, as well as bacterial motility proteins, exhibited a decreasing trend over time in microplastic communities.

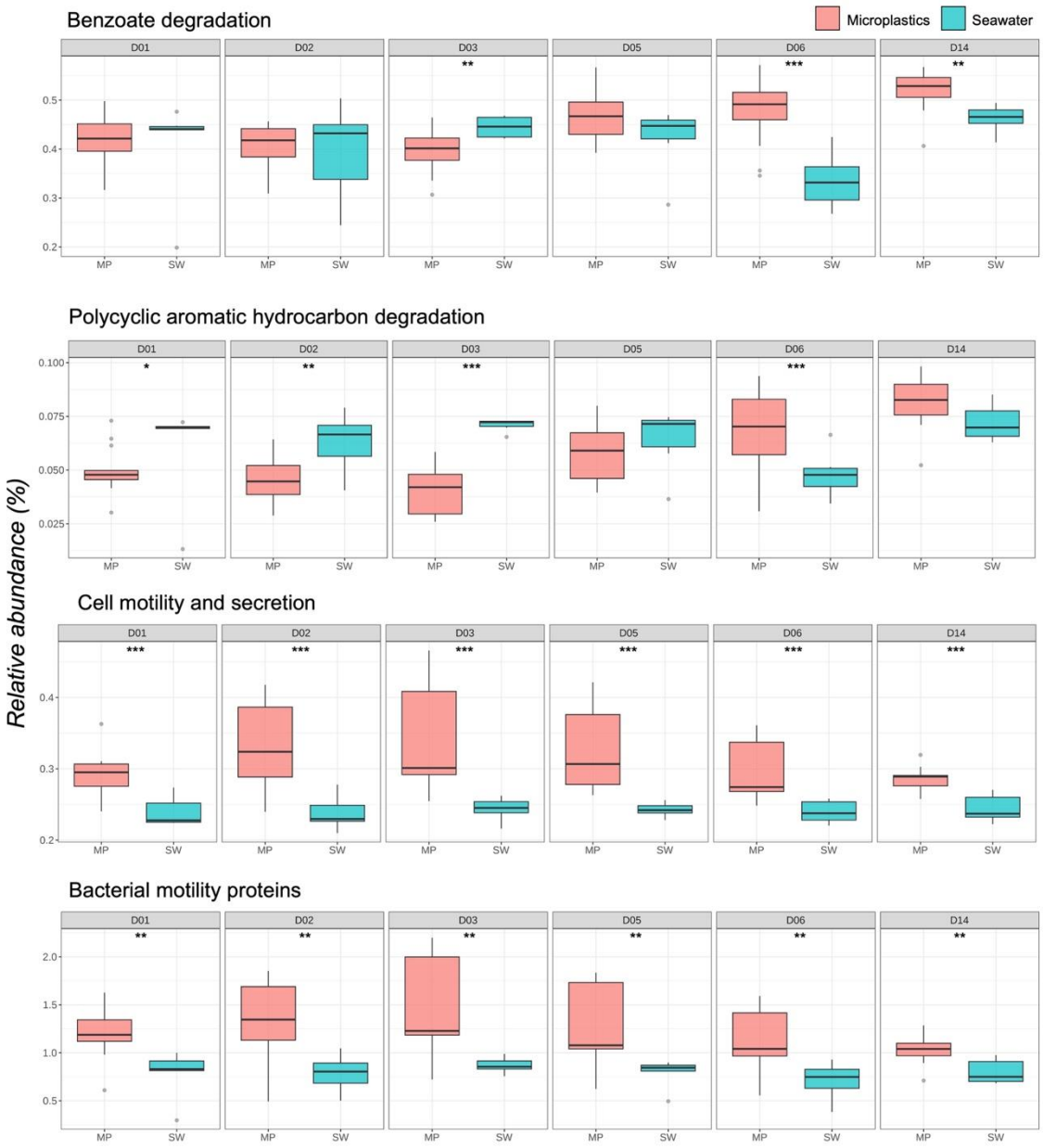

Figure 17. Temporal variation in relative abundance (%) of functional pathways. (* p<0.05, ** p <0.01, *** p <0.001)

3.3.4. Correlation with Environmental Parameters

The correlation coefficient matrix among the environmental parameters was presented in Figure 18a. The results revealed that temperature exhibited a positive correlation with pH, ammonium (NH_4), phosphate (PO_4), and silicate (SiO_2), but a strong negative correlation with salinity. Additionally, salinity showed a negative correlation with macronutrient factors. Furthermore, pH showed a positive correlation with NH_4, while NH_4 displayed a strong positive correlation with PO_4. Moreover, SiO_2 was positively correlated with PO_4. The correlation analysis between environmental parameters and relative abundance of dominant taxa (top 10 with the highest relative abundance) in the microplastic samples was depicted in Figure 18b. The results showed that temperature exhibited a positive correlation with *Crocinitomicaceae*, *Cryomorphaceae*, and *Cyclobacteriaceae*, while showing a negative correlation with *Saprospiraceae* and *Rhizobiaceae*. Salinity demonstrated a positive correlation with *Rhodobacteraceae*, *Saprospiraceae*, and *Rhizobiaceae*. Furthermore, pH showed a positive correlation with *Rhodobacteraceae* but a negative correlation with *Vibrionaceae*. Notably, NH_4 and PO_4 exhibited a negative correlation with *Cyclobacteriaceae*. Moreover, SiO_2 showed a negative correlation *Rhodobacteraceae*, *Saprospiraceae*, and *Rhizobiaceae*, while presenting a positive correlation with *Saccharospirillaceae*, *Oleiphilaceae*, *Vibrionaceae*, and *Cryomorphaceae*. Overall, these findings suggested a significant correlation between the relative abundance of dominant taxa of microplastic community and the environmental factors.

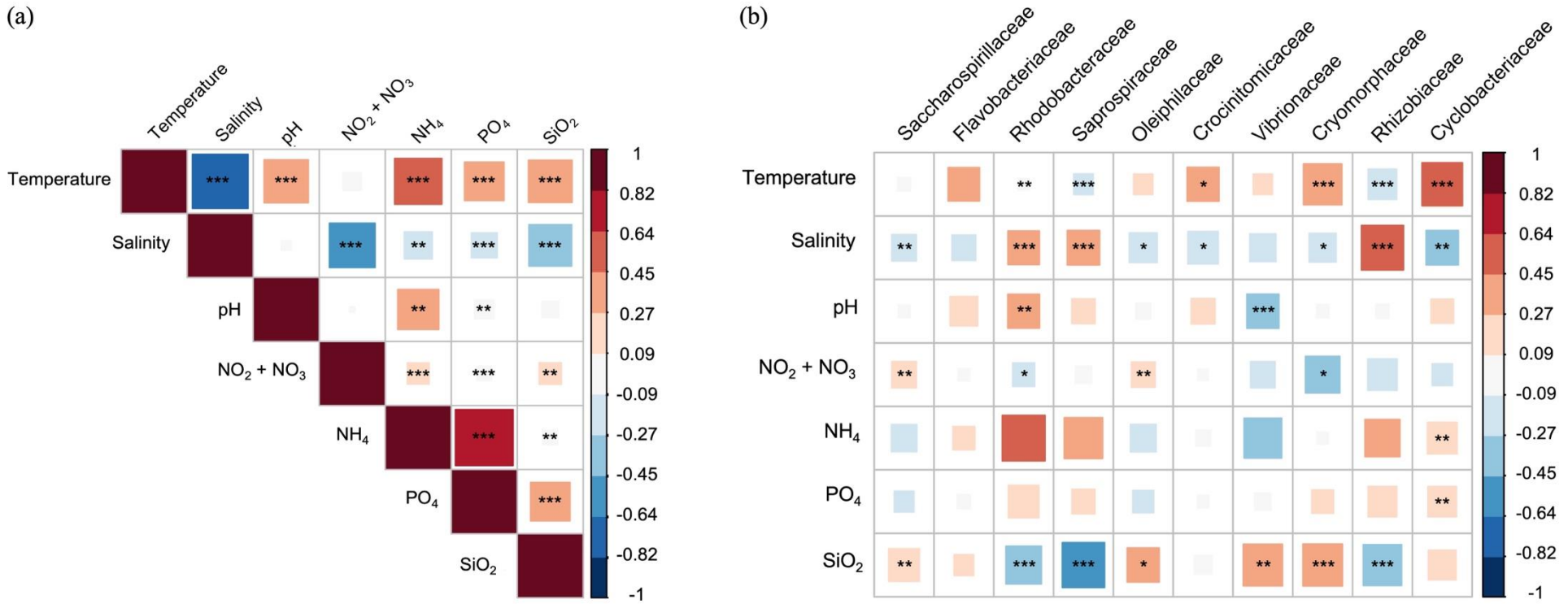

Figure 18. Correlation coefficient matrix of environmental parameters. Pairwise comparison among the environmental parameters (a) and between environmental parameters and dominant taxa (top 10 with the highest relative abundance) at the family level in the microplastic samples (b). Positive correlations are represented by red color, while negative correlations are indicated by blue color. The intensity of the color reflects the strength of the correlation. (* p<0.05, ** p <0.01, *** p <0.001)

4. Discussion

4.1. Diversity of Prokaryotic Communities

4.1.1. Alpha Diversity

In this study, there was no statistically significant difference in alpha diversity between microplastics and the surrounding seawater, although variation of the microplastic samples was higher than bulk seawater samples. This finding was consistent with previous research that reported no significant difference between microplastic and seawater communities in alpha diversity during the early stages (1 week) (Zhang et al. 2022). The development and temporal patterns of early biofilm communities were influenced by various factors, such as the properties of the substrate, hydrographic conditions, nutrient availability, and the presence of free-living microbial communities (Datta et al. 2016; Qian et al. 2022).

4.1.2. Beta Diversity

This study revealed significant differences in beta diversity based on Bray-Curtis dissimilarity and major taxonomic composition, showing the differentiation between microplastic-associated communities and bulk seawater communities. Consistent with these findings, previous studies have consistently reported plastisphere microbial communities were clearly differentiated from the surrounding seawater (Basili et al. 2020; Frère et al. 2018; Zettler et al. 2013; Zhang et al. 2022). However, intriguingly, the particle-attached communities exhibited partial clustering in the microplastic community on Day 1 and Day 2. In the study by Hou et al. (Hou et al. 2021), the particle-attached sample was further classified into LPA (Large Particle Attached, >20 μm) and SPA (Small Particle Attached, 2–20 μm), and it was observed that the microplastic community clustered with the LPA fraction. Therefore, the clustering of the particle-attached community with microplastic community at the Day 1–2 suggested a higher probability of the prokaryotic communities associated with particles larger than 20 μm.

Furthermore, the community structure of microplastic was found to be influenced more by exposure time than by polymer type. When considering the results of ANOSIM based on Bray-Curtis dissimilarity (Table 5), ANOSIM analysis based on UniFrac distance, and NMDS plot (data not shown), the differences between polymer types were not clearly distinguished. These results were consistent with the findings of previous studies, suggesting that polymer type has a lesser impact compared to other factors (Basili et al. 2020; Dudek et al. 2020; Kesy et al. 2019; Wu et al. 2020). However, pairwise comparisons between PP and HIPS, as well as between PP and GPPS, showed relatively higher R-values (R=0.457 and R=0.517, respectively) compared to comparisons between other polymer types. It was important to note that the absence of PP data on Day 14, due to sample loss, could potentially lead to misinterpretation when comparing PP with other polymer types. On the other hand, pairwise comparisons based on exposure time revealed significant differences when comparing the Day 14 with other time points (R=0.584–0.848, p=0.001). The influence of exposure time on the distinct structure of microplastic communities has also been reported in previous studies (Latva et al. 2022; Li et al. 2020).

4.2. Differences in Taxonomic Composition and Major ASVs

4.2.1. Microplastic Communities and Seawater Communities

Significant differences in taxonomic composition were observed between the microplastic-associated communities and the surrounding bulk seawater communities. At the order level, Flavobacteriales, Oceanospirillales, and Rhodobacterales were the dominant taxonomic groups in the microplastic communities, whereas Flavobacteriales, Rhodobacterales, and SAR11 clade were prevalent in the bulk seawater. These findings are consistent with previous study (Dudek et al. 2020; Zhang et al. 2022) and support the notion that specific taxonomic patterns were associated with microplastic environments.

Although microplastic communities and surrounding seawater communities exhibited differences, some similar taxa in community composition were observed. The taxonomic analysis and major ASV analysis revealed that Synechococcales were relatively abundant in the bulk seawater community compared to the microplastic community. However, they were still detected within the microplastic-associated communities. This suggests that pioneer colonizers on plastic, such as photosynthetic microorganisms like diatoms and cyanobacteria, may have influenced the presence of Synechococcales (Antunes et al. 2020). The distinction between particle-attached communities and free-living communities has been reported about bacterial lifestyles. (DeLong et al. 1993; Zhang et al. 2007). As a result, microbial communities with a tendency for particle attachment are likely to attach to microplastics as well. The bacterial taxa such as Vibrionales and Rhizobiales, which are known for their attachment to particles, exhibit higher relative abundance within microplastic communities compared to the surrounding seawater communities. Interestingly, within these taxa, the particle-attached fraction demonstrates higher relative abundance values compared to the free-living fraction, indicating a stronger association with particle attachment (Zhang et al. 2007).

4.2.2. Taxonomic Composition and Major ASVs of Microplastic-Associated Prokaryotic Communities

The dominant taxa of microplastic communities were Bacteroidia (36.53±15.54 %), Gammaproteobacteria (27.45±21.39 %) and Alphaproteobacteria (26.00±15.63 %) at the class level. Additionally, Alphaproteobacteria were found to be increased over time, while Gammaproteobacteria showed a decreasing trend. These pioneer communities were rapidly succeeded by Alphaproteobacteria. (Du et al. 2022; Oberbeckmann et al. 2015; Pollet et al. 2018). The dominant taxa of microplastic communities were Flavobacteriales (30.51±13.20 %), Oceanospirillales (19.40±21.40 %), and Rhodobacterales (19.16±13.36 %) at the order level. Additionally, *Flavobacteriaceae* (21.60±10.36 %), *Rhodobacteraceae* (19.29±13.47 %), and *Saccharospirillaceae* (14.73±17.49 %) taxa comprised of microplastic communities at the family level. Furthermore, the LEfSe analysis revealed that these taxa were uniquely associated with microplastic communities, indicating their specific presence in microplastic communities (Figures 15 and 16). These taxa commonly represented in microplastic-associated communities (Dudek et al. 2020; Pollet et al. 2018; Vaksmaa et al. 2021). Furthermore, a higher proportion of the major ASVs observed in the prokaryotic communities of microplastics were found to be affiliated with taxa such as *Saccharospirillaceae, Oleiphilaceae, Rhodobacteraceae,* and *Flavobacteriaceae* (Figures 13 and 14). These taxa were prominently represented and played a significant role in shaping the taxonomic structure of microplastic communities. In addition, the ASVs belonging to these taxa showed a decreasing trend over time. ASV 4493 (*Pseudofulvibacter* sp.), ASV 4471 (*Winogradskyella* sp.), and ASV 4387 (*Tenacibaculum* sp.) were observed to be lower relative abundance at the Day 14, although keeping relative abundance higher not until Day 14. Moreover, ASV 8693 (*Pseudahrensia* sp.), ASV 8067 (*Rhodobacter* sp.), ASV 8004 (*Planktotalea* sp.), ASV 7811 (*Rhodobacteraceae*; unknown genus sp.), and ASV 7795 (*Rhodobacteraceae*; unknown genus sp.) tended to increase relative abundance over time. These taxa, except for ASV 8693, were well-known as core members of microplastic communities and were affiliated with Alphaproteobacteria (Pollet et al. 2018).

Moreover, distinct taxonomic compositions were observed based on the polymer types.

Specifically, the relative abundance of *Oleiphilaceae* taxa was higher in HIPS and GPPS compared to other polymer types. Oceanospirillales taxa were found across various polymer types, with HDPE and PP polymer types exhibiting relatively lower proportions compared to other polymer types. Vibrionales were observed to be enriched in microplastic samples, and notably, the PP sample exhibited a higher relative abundance compared to other plastic types. This finding aligns with previous studies reporting the prevalence of Vibrionales in plastic-associated environments (Kesy et al. 2020). These results of difference among the polymer types indicated that microbial selection of plastic may contribute to this observation (Amaral-Zettler et al. 2020; Yang et al. 2020).

ASV 11829 (*Oceaniserpentilla* sp.), ASV 11715, 11713, 11710 (*Oleibacter* sp.), ASV 11609, 11596 (*Oleiphilus* sp.), ASV 4471 (*Winogradskyella* sp.), ASV 4387,4385, 4337 (*Tenacibaculum* sp.), and ASV 855 (*Clostridium* sp.) were belonged in bacterial genera with members involved in Obligate hydrocarbonoclastic bacteria (OHCB) (Prince et al. 2010; Vaksmaa et al. 2021; Yakimov et al. 2007). These findings indicated that microorganisms capable of plastic degradation may selectively target plastic materials in the early stages. Additionally, biodegrading microbes (BD) have the potential to initiate the colonization of surfaces, particularly when carbon and energy sources such as oligomers and plastic additives are present (Wright et al. 2020).

Consistent with these findings, the functional inference analysis supported the results that functions related to cell motility decreased over time (Figure 17). This suggests that the initial attachment to submerged materials, particularly plastics, was influenced by pioneer colonizers. Additionally, it was predicted that the degradation function of substances such as polycyclic aromatic hydrocarbon (PAH) and benzoate would increase over time (Figure 17). Jiang et al. (Jiang et al. 2018) conducted a sample collection of plastics (it could be aged plastics) and observed a deficiency in metabolic pathways and genes, such as "cell motility," which corresponded to the attached lifestyle typically observed in plastic-associated communities. In contrast, the pathway of xenobiotics biodegradation and metabolism were enriched, consistent with previous studies (Jiang et al. 2018; Xu et al. 2019).

4.3. Limitations and Future Study

This study had inherent limitations due to in situ incubation experiments. Microplastic pellets were placed inside a stainless cage with a mesh size of 1.2 mm for in situ incubation. This setup had limitations in terms of receiving less sunlight than the actual environment and being unable to assess the influences of organisms larger than 1.2 mm. Latva et al. (Latva et al. 2022) demonstrated that sunlight influences the initial microbial communities on microplastics. Pinto et al. (Pinto et al. 2019) revealed that the light regime not only affects heterotrophic bacteria but also the entire microbial community. Additionally, to investigate the plastisphere community structure, stainless steel cages were used, which was expected to have minimal bias of materials. However, at the Day 14 time point, corrosion was observed at the edges of the cages. This unexpected corrosion could potentially impact the composition of the prokaryotic communities under study. Furthermore, due to such corrosion on the cages, the connecting line for the PP sample at Day 14 was severed, resulting in the loss of samples and the inability to compare the communities among different polymer types to the PP sample.

Furthermore, in this study, there exists a gap concerning substrates other than plastic. Previous studies on microbial biofilms communities compared not only plastic substrates but also various other substrates (Kesy et al. 2019; Oberbeckmann et al. 2016; Zhang et al. 2022; Zhao et al. 2021). For instance, in the study conducted by Oberbeckmann et al. (Oberbeckmann et al. 2016), no significant difference was observed in the microbial community structure between plastic (PET) and glass substrates. However, in the research carried out by Zhang et al. (Zhang et al. 2022), the microbial communities were differentiated between plastic substrates and natural substrates (wood and shell). These results showed the importance of investigating the microbial dynamics on different types of substrates beyond plastic to gain a comprehensive understanding of the ecological implications.

Moreover, this study conducted subsampling of in situ experiments at Day 1, 2, 3, 5, 6, and 14, but there existed a gap in information on prokaryotic community changes between Day 6 and Day 14. Based on the analysis of beta diversity and taxonomic composition, it was evident that the prokaryotic communities at Day 6 and Day 14 exhibited significant differences, indicating the

necessity for further investigation during that time interval.

Moreover, previous studies showed that there were significant changes in plastic community composition after one month (Dudek et al. 2020; Li et al. 2020; Zhang et al. 2022). Additionally, according to Hou et al. (Hou et al. 2021), a comparison of seawater fraction and microplastic communities during day 15 and day 90 (sampling time points; day 15, 30, 60, and 90) demonstrated a decrease in the dissimilarity between the seawater and microplastic communities, indicating similar communities between microplastic and seawater fraction over time. These previous results showed the importance of large time scale studies comparing early–stage communities to late–stage communities.

5. Conclusions

This study investigated the prokaryotic community structure and characteristics during the initial stages of microplastic biofilm formation in coastal seawater using in situ incubation experiment. The findings revealed a clear distinct differentiation between microplastic-associated prokaryotic communities and bulk seawater communities. Specifically, the Bray-Curtis dissimilarities between prokaryotic communities in bulk seawater and microplastics were highest at Day 14, indicating significant shifts in community composition over time. The microplastic-associated prokaryotic communities were influenced by exposure time based on Bray-Curtis dissimilarity distance. Furthermore, the predominant taxa observed in microplastic communities at the order level were Oceanospirillales, Rhodobacterales, and Flavobacteriales. Notably, the major amplicon sequence variants (ASVs) identified in microplastic communities were associated with obligate hydrocarbonoclastic bacteria (OHCB), and their relative abundances exhibited temporal variations. The results reveal that the initial prokaryotic communities showed dynamic characteristics, characterized by fluctuations in composition and structure. Overall, this study offers insights into the formation of microplastic biofilms during the initial stages and establishes a baseline for understanding the mechanisms underlying microbial microplastic biofilm formation.

References

Amaral-Zettler LA, Zettler ER, Mincer TJ. 2020. Ecology of the plastisphere. *Nat. Rev. Microbiol.* 18(3):139–51

Andrews S. 2010. FastQC: a quality control tool for high throughput sequence data

Antunes JT, Sousa AGG, Azevedo J, Rego A, Leão PN, Vasconcelos V. 2020. Distinct Temporal Succession of Bacterial Communities in Early Marine Biofilms in a Portuguese Atlantic Port. *Frontiers Microbiol.* 11:1938

Auta HS, Emenike CU, Fauziah SH. 2017. Distribution and importance of microplastics in the marine environment: A review of the sources, fate, effects, and potential solutions. *Environ Int*. 102:165–76

Basili M, Quero GM, Giovannelli D, Manini E, Vignaroli C, et al. 2020. Major Role of Surrounding Environment in Shaping Biofilm Community Composition on Marine Plastic Debris. *Frontiers Mar Sci*. 7:262

Bolger AM, Lohse M, Usadel B. 2014. Trimmomatic: a flexible trimmer for Illumina sequence data. *Bioinformatics*. 30(15):2114–20

Bolyen E, Rideout JR, Dillon MR, Bokulich NA, Abnet CC, et al. 2019. Reproducible, interactive, scalable and extensible microbiome data science using QIIME 2. *Nat Biotechnol*. 37(8):852–57

Callahan BJ, McMurdie PJ, Rosen MJ, Han AW, Johnson AJA, Holmes SP. 2016. DADA2: High-resolution sample inference from Illumina amplicon data. *Nature methods*. 13(7):581–83

Dang H, Lovell CR. 2000. Bacterial Primary Colonization and Early Succession on Surfaces in Marine Waters as Determined by Amplified rRNA Gene Restriction Analysis and Sequence Analysis of 16S rRNA Genes. *Appl Environ Microb*. 66(2):467–75

Dang H, Lovell CR. 2016. Microbial Surface Colonization and Biofilm Development in Marine Environments. *Microbiol Mol Biol R*. 80(1):91–138

Datta MS, Sliwerska E, Gore J, Polz MF, Cordero OX. 2016. Microbial interactions lead to rapid micro-scale successions on model marine particles. *Nat. Commun.* 7(1):11965

DeLong EF, Franks DG, Alldredge AL. 1993. Phylogenetic diversity of aggregate-attached vs. free-living marine bacterial assemblages. *Limnology and oceanography*. 38(5):924–34

Douglas GM, Maffei VJ, Zaneveld JR, Yurgel SN, Brown JR, et al. 2020. PICRUSt2 for prediction of metagenome functions. *Nat Biotechnol*. 38(6):685–88

Du Y, Liu X, Dong X, Yin Z. 2022. A review on marine plastisphere: biodiversity, formation, and role in degradation. *Comput. Struct. Biotechnol. J.* 20:975–88

Dudek KL, Cruz BN, Polidoro B, Neuer S. 2020. Microbial colonization of microplastics in the Caribbean Sea. *Limnology Oceanogr Lett*. 5(1):5–17

Frère L, Maignien L, Chalopin M, Huvet A, Rinnert E, et al. 2018. Microplastic bacterial communities in the Bay of Brest: Influence of polymer type and size. *Environ Pollut*. 242(Pt A):614–25

Frias JPGL, Nash R. 2019. Microplastics: Finding a consensus on the definition. *Mar Pollut Bull*. 138:145–47

Hou D, Hong M, Wang K, Yan H, Wang Y, et al. 2021. Prokaryotic community succession and assembly on different types of microplastics in a mariculture cage. *Environ Pollut*. 268(Pt A):115756

Jiang P, Zhao S, Zhu L, Li D. 2018. Microplastic-associated bacterial assemblages in the intertidal zone of the Yangtze Estuary. *Sci. The Total. Environ.* 624:48–54

Kesy K, Labrenz M, Scales BS, Kreikemeyer B, Oberbeckmann S. 2020. Vibrio Colonization Is Highly Dynamic in Early Microplastic-Associated Biofilms as Well as on Field-Collected Microplastics. *Microorganisms*. 9(1):76

Kesy K, Oberbeckmann S, Kreikemeyer B, Labrenz M. 2019. Spatial Environmental Heterogeneity Determines Young Biofilm Assemblages on Microplastics in Baltic Sea Mesocosms. *Front Microbiol*. 10:1665

Latva M, Dedman CJ, Wright RJ, Polin M, Christie-Oleza JA. 2022. Microbial pioneers of plastic colonisation in coastal seawaters. *Mar Pollut Bull*. 179:113701

Li J, Huang W, Jiang R, Han X, Zhang D, Zhang C. 2020. Are bacterial communities associated with microplastics influenced by marine habitats? *Sci Total Environ*. 733:139400

Martin M. 2011. Cutadapt removes adapter sequences from high-throughput sequencing reads. *EMBnet. journal*. 17(1):10–12

McMurdie PJ, Holmes S. 2013. phyloseq: An R Package for Reproducible Interactive Analysis and Graphics of Microbiome Census Data. *Plos One*. 8(4):e61217

Oberbeckmann S, Löder MGJ, Labrenz M. 2015. Marine microplastic-associated biofilms – a review. *Environ Chem*. 12(5):551–62

Oberbeckmann S, Osborn AM, Duhaime MB. 2016. Microbes on a Bottle: Substrate, Season and Geography Influence Community Composition of Microbes Colonizing Marine Plastic Debris. *Plos One*. 11(8):e0159289

Parada AE, Needham DM, Fuhrman JA. 2016. Primers for marine microbiome studies. *Environ Microbiol*. 18(5):1403–14

Parsons TR, Maita Y, Lalli CM. 1984. *A Manual of Chemical and Biological Methods for Seawater Analysis*. Pergamon Press, NewYork, NY, USA

Pinto M, Langer TM, Hüffer T, Hofmann T, Herndl GJ. 2019. The composition of bacterial communities associated with plastic biofilms differs between different polymers and stages of biofilm succession. *PLoS ONE*. 14(6):e0217165

PlasticsEurope. 2019. Plastics—The Facts 2019: An Analysis of European Plastics Production, Demand and Waste Data, PlasticsEurope

Pollet T, Berdjeb L, Garnier C, Durrieu G, Poupon CL, et al. 2018. Prokaryotic community successions and interactions in marine biofilms: the key role of Flavobacteriia. *Fems Microbiol Ecol*. 94(6):

Prince RC, Gramain A, McGenity TJ. 2010. Prokaryotic Hydrocarbon Degraders. , pp. 1669–92. Berlin, Heidelberg: Springer Berlin Heidelberg

Qian P-Y, Cheng A, Wang R, Zhang R. 2022. Marine biofilms: diversity, interactions and biofouling. *Nat Rev Microbiol*. 20(11):671–84

RCoreTeam. 2022. R: A Language and Environment for Statistical Computing

Segata N, Izard J, Waldron L, Gevers D, Miropolsky L, et al. 2011. Metagenomic biomarker discovery and explanation. *Genome Biol*. 12(6):R60

Shibata A, Goto Y, Saito H, Kikuchi T, Toda T, Taguchi S. 2006. Comparison of SYBR Green I and SYBR Gold stains for enumerating bacteria and viruses by epifluorescence microscopy. *Aquat. Microb. Ecol.* 43:223–31

Vaksmaa A, Knittel K, Asbun AA, Goudriaan M, Ellrott A, et al. 2021. Microbial Communities on Plastic Polymers in the Mediterranean Sea. *Front Microbiol*. 12:673553

Wayman C, Niemann H. 2021. The fate of plastic in the ocean environment – a minireview. *Environ. Sci. Process. Impacts*. 23(2):198–212

Wei T, Simko V. 2021. package "corrplot": Visualization of a Correlation Matrix. 2017

Wen B, Liu J-H, Zhang Y, Zhang H-R, Gao J-Z, Chen Z-Z. 2020. Community structure and functional diversity of the plastisphere in aquaculture waters: Does plastic color matter? *Sci Total Environ*. 740:140082

Wickham H, Wickham H. 2016. Data analysis. . 189–201

Wright RJ, Erni-Cassola G, Zadjelovic V, Latva M, Christie-Oleza JA. 2020. Marine Plastic Debris: A New Surface for Microbial Colonization. *Environ. Sci. Technol.* 54(19):11657–72

Wu N, Zhang Y, Zhao Z, He J, Li W, et al. 2020. Colonization characteristics of bacterial communities on microplastics compared with ambient environments (water and sediment) in Haihe Estuary. *Sci. The Total. Environ.* 708:134876

Xu X, Wang S, Gao F, Li J, Zheng L, et al. 2019. Marine microplastic-associated bacterial community succession in response to geography, exposure time, and plastic type in China's coastal seawaters. . 145:278–86

Yakimov MM, Timmis KN, Golyshin PN. 2007. Obligate oil-degrading marine bacteria. *Curr. Opin. Biotechnol.* 18(3):257–66

Yang Y, Liu W, Zhang Z, Grossart H-P, Gadd GM. 2020. Microplastics provide new microbial niches in aquatic environments. *Appl. Microbiol. Biotechnol.* 104(15):6501–11

Zettler ER, Mincer TJ, Amaral-Zettler LA. 2013. Life in the "Plastisphere": Microbial Communities on Plastic Marine Debris. *Environ Sci Technol*. 47(13):7137–46

Zhang R, Liu B, Lau SC, Ki J-S, Qian P-Y. 2007. Particle-attached and free-living bacterial communities in a contrasting marine environment: Victoria Harbor, Hong Kong. *FEMS microbiology ecology*. 61(3):496–508

Zhang S-J, Zeng Y-H, Zhu J-M, Cai Z-H, Zhou J. 2022. The structure and assembly mechanisms of plastisphere microbial community in natural marine environment. *J Hazard Mater*. 421:126780

Zhao S, Zettler ER, Amaral-Zettler LA, Mincer TJ. 2021. Microbial carrying capacity and carbon biomass of plastic marine debris. *The ISME J.* 15(1):67–77

Abstract in Korean

해양 내 플라스틱은 다양한 미생물에 의해 빠르게 부착되며, 해양 미생물에게 서식지를 제공한다. 기존 연구는 해양 내 미세플라스틱을 수집하여 미세플라스틱에 서식하는 미생물 군집에 대한 연구가 수행되었다. 미세플라스틱에 서식하는 미생물 군집은 노출 시간에 영향을 받을 수 있다는 것을 시사했다. 그러나 초기 미세플라스틱 원핵생물 군집 구조에 대한 연구는 현재까지 부족한 실정이다. 따라서 본 연구는 연안 해수에서 다섯 가지 재질의 미세플라스틱에 대한 현장 배양 실험을 통해 초기(1–14 일) 미세플라스틱 생물막의 원핵생물 군집 구조와 특성을 조사하였다. 16S rRNA 유전자를 기반한 차세대 염기서열 분석을 통해 미세플라스틱 생물막 형성에 대한 원핵생물 군집 구조와 특성을 밝혀냈다. 미세플라스틱 군집과 주변 환경 해수 군집은 확연히 구분되었다. 또한 미세플라스틱 군집은 미세플라스틱의 재질보다 노출 시간에 영향을 받는 것으로 나타났다. 특히 미세플라스틱 군집에서 확인된 주요 ASV 는 OHCB (Obligate Hydrocarbonoclastic Bacteria)와 관련되어 있었으며, 미세플라스틱 재질에 따라 특이적으로 나타나는 ASV 도 존재했다. 또한 일부 미세플라스틱 군집의 주요 분류군의 상대 풍부도는 시간에 따라 변화하였다. 더 나아가 미세플라스틱 군집에서 벤조산 및 다환 방향족 탄화수소를 분해하는 대사 경로는 시간이 지남에 따라 증가하는 것으로 나타났다. 이러한 결과는 초기 미세플라스틱 원핵생물 군집 구조와 기능은 시간적 변동성을 가진다는 것을 보여주었다. 본 연구는 초기 미세플라스틱 원핵생물 군집 조성에 대한 이해와 생물막 형성 메커니즘을 이해하기 위한 기초 지식을 제공하며, 더 나아가 해양 미세플라스틱 오염에 대한 향후 연구에 기여할 수 있다.

주요어 : 미세플라스틱, 초기 생물막, 원핵생물 군집, 현장 배양 실험, 차세대 염기서열 분석법

학번 : 2021-20686